Continuous estimation of anthropogenic CO_2: Model-based evaluation of CO_2, CO, $\delta^{13}C(CO_2)$ and $\Delta^{14}C(CO_2)$ tracer methods

S.N. Vardag[1], C. Gerbig[2], G. Janssens-Maenhout[3], I. Levin[1]

[1]{Institut für Umweltphysik, Heidelberg University, Germany}

[2]{Max Planck Institute for Biogeochemistry, Hans-Knöll-Str.10, 07745 Jena, Germany}

[3]{European Commission, Joint Research Centre, Ispra, Via Fermi, 2749, 21027 Ispra, Italy}

Correspondence to: S.N. Vardag (svardag@iup.uni-heidelberg.de)

Abstract

We investigate different methods for estimating anthropogenic CO_2 using modelled continuous atmospheric concentrations of CO_2 alone, as well as CO_2 in combination with the surrogate tracers CO, $\delta^{13}C(CO_2)$ and $\Delta^{14}C(CO_2)$. These methods are applied at three hypothetical stations representing rural, urban and polluted conditions. We find that independent of the tracer used, an observation-based estimate of continuous anthropogenic CO_2 is not yet feasible at rural measurement sites due to the low signal to noise ratio of anthropogenic CO_2 estimates at such settings. The tracers $\delta^{13}C(CO_2)$ and CO provide an accurate possibility to determine anthropogenic CO_2 continuously, only if all CO_2 sources in the catchment area are well characterized or calibrated with respect to their isotopic signature and CO to anthropogenic CO_2 ratio. We test different calibration strategies for the mean isotopic signature and CO to CO_2 ratio using precise $\Delta^{14}C(CO_2)$ measurements on monthly-integrated as well as on grab samples. For $\delta^{13}C(CO_2)$, a calibration with annually averaged $^{14}C(CO_2)$ grab samples is most promising, since integrated sampling introduces large biases into anthropogenic CO_2 estimates. For CO, these biases are smaller. The precision of continuous anthropogenic CO_2 determination using $\delta^{13}C(CO_2)$ depends on measurement precision of $\delta^{13}C(CO_2)$ and CO_2 while the CO-method is mainly limited by the variation of natural CO sources and sinks. At present, continuous anthropogenic CO_2 could be determined using the tracers $\delta^{13}C(CO_2)$ and/or CO with a precision of about 30%, a mean bias of about 10% and without significant diurnal discrepancies. Hypothetical future measurements of continuous $\Delta^{14}C(CO_2)$ with a precision of 5 ‰ are promising for anthropogenic CO_2 determination (precision ca. 10-20 %) in future but they are not available yet. The investigated tracer-based approaches open the door to

improving, validating and reducing biases of highly resolved emission inventories using atmospheric observation and regional modelling.

1. Introduction

Earth's carbon budget is strongly influenced by anthropogenic CO_2 emissions into the atmosphere (Keeling et al., 1996, Le Quéré et al., 2015). In order to support studies of the carbon cycle and to determine net and gross carbon fluxes quantitatively, various measurement sites monitor the atmospheric CO_2 mole fraction worldwide. In top-down approaches and in conjunction with atmospheric transport models, these CO_2 measurements are used to infer total CO_2 emissions (Bousquet et al., 2000; Gurney et al., 2002; Peylin et al., 2013), but a differentiation into biogenic, oceanic and anthropogenic CO_2 sources and sinks is not feasible with CO_2 concentration measurements alone. Inverse model studies commonly utilize anthropogenic CO_2 emission inventories to estimate anthropogenic CO_2 and are then able to separate anthropogenic from biogenic or oceanic carbon sink and source influences. However, currently available emission inventories exhibit large discrepancies between each other of about 10-40% at the country level (Peylin et al., 2011), and increase further with decreasing spatial scale (Gurney et al., 2005). These discrepancies suggest that biases may be in the order of about 70-100 % for highly resolved (0.1°x0.1°) data sets and uncertainties (1σ) of emission inventories may be between 30-150 % (Wang et al., 2013). In order to better study and quantify the biospheric carbon fluxes, their underlying processes and potential feedbacks, it is desirable to reduce the current uncertainties as well as biases of emission inventories. Validation and improvement of emission inventories requires accurate and precise anthropogenic CO_2 estimates (as well as accurate and precise transport models) on all relevant time scales ranging from hours to years. We hereafter refer to anthropogenic CO_2 as fuel CO_2 and include non-combustion emissions such as emissions from cement industry or non-energy use of fuels as well as agricultural waste burning. Fossil fuel CO_2 excludes all contributions from biofuel emissions or from agricultural waste burning. We define biofuel CO_2 as non-fossil fuel CO_2 released during combustion, including solid (e.g. wood, waste, charcoal, municipal renewable waste, bagasse, vegetal waste and dung), liquid (e.g. biodiesel, bio gasoline and black liquor) and gaseous (from compost or cattle farm) biomaterial. It does not include large-scale biomass burning. For some purposes e.g., when validating fossil fuel emission reductions, it may actually be advantageous to estimate only the fossil fuel CO_2 contribution, which is the fuel CO_2 contribution without biofuel CO_2. However, when solving for biospheric fluxes, the biofuel CO_2 is important as well, since it equally contributes to the instantaneously measured CO_2 concentration and needs to be separated from the biospheric flux. In the following, we seek to constrain the fuel CO_2 (fossil fuel CO_2 plus biofuel CO_2).

^{14}C measurements are commonly used as surrogate to differentiate between biogenic and fossil fuel CO_2 contributions in the atmosphere, since fossil fuels do not contain any ^{14}C, in contrary to biogenic sources (Levin et al., 2003). The $^{14}C/C$ isotope ratio in CO_2 is expressed on the $\Delta^{14}C(CO_2)$ scale, which denotes the deviation of the $^{14}C/C$ ratio in CO_2 from a standard material in permil (Stuiver and Polach, 1977). We use the depletion of $\Delta^{14}C(CO_2)$ at a polluted measurement site relative to $\Delta^{14}C(CO_2)$ in clean background air to derive quantitative information on the contribution of fossil fuel CO_2 to total measured CO_2 mole fraction at the polluted site. Radiocarbon (^{14}C) is thus used as quantitative tracer for fossil fuel contributions (e.g. Levin et al., 2003; Levin and Karstens, 2007; Turnbull et al., 2006; Turnbull et al., 2015). However, there are a number of problems, when using $^{14}C(CO_2)$ as tracer for anthropogenic emissions: First, precise $\Delta^{14}C(CO_2)$ measurements from conventional counting or accelerator mass spectrometry (AMS) (better than 2 ‰) are time and cost intensive, thus currently prohibiting the coverage of large periods and large area of such measurements. Attempts have been made to sample $^{14}C(CO_2)$ with a higher measurement frequency using gas chromatography (GC) coupled to continuous-flow AMS (McIntyre et al., 2013), but the technique is not applicable to atmospheric ^{14}C samples so far and the precision in $\Delta^{14}C(CO_2)$ is lower than for AMS or conventional counting. This results in less precise fossil fuel CO_2 estimates. These studies indicate, however, that the measurement precision using GC and continuous-flow AMS may reach 5 ‰ in future. The benefit of such hypothetical quasi-continuous but reduced precision fossil fuel CO_2 estimates is assessed for the first time in this work in order to check if these measurements would provide beneficial constraints for determining CO_2 continuously.

Second, a complication of applying $\Delta^{14}C(CO_2)$ measurements for fossil fuel CO_2 estimation is that nuclear power plants as well as nuclear fuel reprocessing plants emit $^{14}C(CO_2)$ and can bias regional $\Delta^{14}C(CO_2)$-based estimates of fossil fuel contributions if not taken into account (Levin et al., 2003; Graven and Gruber, 2011, Vogel et al., 2013b). Moreover, biofuel CO_2 contributions cannot be monitored with $\Delta^{14}C(CO_2)$ measurements, since they have a similar $\Delta^{14}C(CO_2)$ signature as the biosphere or may even be elevated in ^{14}C due to the bomb radiocarbon $^{14}C(CO_2)$ stored in wood material. This could become especially problematic, since the use of biofuels is expected to play an increasingly important role for the energy supply in the near future (Coyle, 2007). Recognizing these shortcomings of $\Delta^{14}C(CO_2)$ as tracer for anthropogenic CO_2, it is worth considering other tracers for the estimation of fuel CO_2 contributions.

Turnbull et al. (2015) have shown that for an urban study area in the middle of the North American continent, the local CO_2 offset relative to clean air, ΔCO_2, can be used as tracer for fuel CO_2 contributions, if all other CO_2 sources and sinks, such as from the living biosphere, are negligible. This may be the case for wintertime periods in urban areas when using a background station upwind and close to the urban area. However, we do not expect ΔCO_2 to be a quantitative tracer when biospheric fluxes occur within the study area. This is normally the case in spring, summer and autumn.

Since CO is often co-emitted during (incomplete) combustion and since CO can be measured continuously, the CO offset relative to clean air, ΔCO, is frequently used as tracer for fuel CO_2 (Meijer et al., 1996; Gamnitzer et al., 2006; Rivier et al., 2006; Turnbull et al., 2006; Levin and Karstens, 2007; Vogel et al., 2010, Turnbull et al., 2011; Newman et al., 2013). If the mean ratio of the CO offset (Δx) relative to the fuel CO_2 offset (Δy_F), i.e. $\Delta x/\Delta y_F := \overline{R_F}$, is known and relatively constant within one month, it is principally possible to derive a continuous Δy_F estimate from Δx measurements by dividing Δx by monthly mean $\overline{R_F}$. The overbar shall emphasize that we use one averaged value for R_F, even though it actually varies with the relative fraction of the different emission groups in a varying catchment area of the measurement site. CO is also produced during oxidation of methane and hydrocarbons, particularly during summer (Granier et al., 2000). The main sinks of CO are photo-oxidation and reaction with OH (Parrish et al., 1993) as well as soil uptake (Inman et al., 1971), leading to a rather short atmospheric lifetime of CO of several weeks in summer (Prather et al., 2011). Natural CO sinks and sources vary on time scales of hours to seasons. Further, relative contributions of different fuel CO_2 sectors (e.g. energy production, road traffic, residential heating, industrial emissions etc.) with different emission ratios ($\Delta CO/\Delta CO_2$), may vary on short time scales of hours to longer time scales of years, if e.g. combustion technologies, processes and procedures change in the long-term. Therefore, the mean $\overline{R_F}$ ($=\Delta x/\Delta y_F$) is a function of space and time and might need to be calibrated using e.g. $\Delta^{14}C(CO_2)$ measurements

(Levin and Karstens, 2007). If $\overline{R_\mathrm{F}}$ does not vary significantly within the time scale of the calibration, continuous Δy_F can be estimated. However, if $\overline{R_\mathrm{F}}$ varies strongly on time scales of smaller than the calibration interval, further corrections (e.g. diurnal or seasonal) may be necessary (Vogel et al., 2010). These corrections are only reliable if $\overline{R_\mathrm{F}}$ variations are systematic. Since this is not always the case, additional or other continuous tracers may need to be considered to improve fuel CO_2 estimates.

One of these tracers may be $\delta^{13}C(CO_2)$, since fuel emissions tend to be more depleted in $^{13}CO_2$ than fluxes from the biosphere. Zondervan and Meijer (1996), Pataki et al. (2006) and Djuricin et al. (2010) have attempted to estimate fuel CO_2 emissions in specific case studies using mass spectrometric measurements of $\delta^{13}C(CO_2)$, in addition to $\Delta^{14}C(CO_2)$ measurements. Recently, new optical instrumentation allows measuring $\delta^{13}C(CO_2)$ continuously (e.g. Esler et al., 2000; Tuzson et al., 2011; Hammer et al., 2013; Vogel et al., 2013a) and thus open the door for $\delta^{13}C(CO_2)$ as a continuous tracer for fuel CO_2 contributions. In order to use $\delta^{13}C(CO_2)$ measurements at an urban site, the mean isotopic signature of the sources (and sinks) in the catchment area of the site, $\overline{\delta_\mathrm{F}}$, must be known and relatively constant and potentially require calibration (as discussed for CO). Further, the signature of fuel CO_2 emissions must be significantly different from biospheric CO_2 emissions in order to differentiate properly between them.

In many settings, we will exhibit neither a constant ratio $\overline{R_\mathrm{F}}$ nor a constant fuel source signature $\overline{\delta_F}$. This will especially be the case if multiple sources (i) with different emission ratios $\overline{R_\mathrm{F,\imath}}$ and different fuel $\delta^{13}C(CO_2)$ source signatures $\delta_\mathrm{F,i}$ are located in the catchment area of the measurement site. In these cases, it may be advantageous to divide the fuel emissions into (two) different groups. CO will only be an adequate tracer for a certain emission group, if this group has a significantly different ratio $\overline{R_\mathrm{F}}$ (=$\Delta x/\Delta y_\mathrm{F}$) than any other emission group. In analogy, $\delta^{13}C(CO_2)$ will only be a good tracer for a certain emission group if the group's emissions are significantly more depleted or enriched with respect to the other groups. If we divide all fuel CO_2 contributions into two emission groups, of which one is well constrained by CO and the other by $\delta^{13}C(CO_2)$, we may then join both tracers to determine the total fuel CO_2 contributions. In several published studies, the CO mole fraction has been used as a tracer for traffic emissions only (e.g. Schmidt et al., 2014), since these often exhibit high $\Delta CO/\Delta CO_2$ ratios. However, in some regions, emission inventories (e.g. Landesamt für Umwelt, Messungen und Naturschutz Baden-Württemberg, available at:

http://www.ekat.baden-wuerttemberg.de/) depict that the emission ratio $\overline{R_{\mathrm{tr}}}$ (=$\Delta x/\Delta y_{\mathrm{tr}}$) has been decreasing during the last decade, degrading CO as a tracer for traffic contributions. At the same time, diesel/petrol for vehicle is blended with an increasing amount of biodiesel/bio gasoline (for OECD countries to the order of 5 %, (IEA, 2014)). More in general, emission inventories show that (the sum of solid, liquid and gaseous) biofuel CO_2 emissions in OECD countries have increased (IEA, 2014) and that the mean emission ratio of biofuel emissions $\overline{R_{\mathrm{bf}}}$ (=$\Delta x/\Delta y_{\mathrm{bf}}$) is very high (EDGARv4.3 emission inventory (EC-JRC/PBL, 2015)), qualifying CO as a tracer for biofuel contributions. However, the emission ratio varies depending on the combustion type. Later we examine separately, if these two emission groups, traffic and biofuel emissions, could possibly be traced with CO.

In the present study, we investigate how continuous CO_2, CO, $\delta^{13}C(CO_2)$ and $\Delta^{14}C(CO_2)$ measurements as well as the combination of these tracers could be used to estimate continuous fuel CO_2. In order to validate how precisely and accurately we may be able to determine fuel CO_2 using continuous (hourly) CO_2, CO, $\delta^{13}C(CO_2)$ and $\Delta^{14}C(CO_2)$as tracers, we use a modelled data set, in which, contrary to measured data sets, CO_2 contributions from all source categories, i.e. the biosphere, from fossil fuel and from biofuel burning are traced separately. Using the modelled mole fractions and isotope records of CO_2, CO, $\delta^{13}C(CO_2)$ and $\Delta^{14}C(CO_2)$, we estimate the total fuel CO_2 offset using these tracers. We then discuss advantages and disadvantages of the different tracers. Using a modelled data set has the additional advantage, that isotopic signatures, emission ratios of different emission sectors etc. can be varied in order to also investigate the sensitivity of these source characteristics on the fuel CO_2 estimate. This enables us to judge how accurately the sources in the catchment of the measurement site need to be characterized for a certain required accuracy of fuel CO_2, and if a calibration, using e.g. precise $\Delta^{14}C(CO_2)$ measurements, is advantageous. In the course of this, we also compare different possible sampling strategies for calibration. We further assess, which measurement precision is needed to achieve continuous fuel CO_2 estimates with sufficient precision. Additionally, we investigate the diurnal cycle of the tracer-based continuous fuel CO_2 estimates and compare them to the modelled reference fuel CO_2 in order to determine if we can reproduce the diurnal cycle correctly and hence, if we would introduce significant biases when using e.g. only afternoon values of fuel CO_2 in inverse models.

We discuss the model results for a three typical European sites with different degrees of pollution, which differ in their annual mean CO_{2F} offset. We define three pollution regimes, which we call "rural", "urban" and "polluted". Rural sites have mean fuel CO_2 offsets of 0-5 μmol/mol. We here use the (hypothetical) station Gartow (53°0' N, 11°3' E) as example with a mean CO_{2F} offset of 3 μmol/mol. Gartow is located in Northern Germany about 160 km north-west of Berlin. Urban sites span a range from 5-20 μmol/mol. We exemplary use Heidelberg, which is a typical urban measurement site with large fuel CO_2 emissions, but also similarly high biogenic sources and sinks in the catchment, which are also active during relatively mild winters. The mean modelled fuel CO_2 offset in Heidelberg is about 16 μmol/mol (24 hours). Polluted sites exhibit annual mean CO_{2F} offsets larger than 20 μmol/mol. A station in the outskirts of Berlin (52°5' N, 13°6' E) is used as example site with modelled mean fuel CO_2 offset of 25 μmol/mol). For all sites, we looked at the same height above ground level (30m a.g.l). Note, that this classification relates only to the mean annual offset and not to single pollution events. We assess, if an estimation of continuous fuel CO_2 is possible at all sites and what may be the best tracer. Finally, we give an outlook on how to apply this model study to a real measured data set. Our investigation aims at providing the basis for the decision if continuous measurements of CO_2, CO, $\delta^{13}C(CO_2)$ and $\Delta^{14}C(CO_2)$ would be worth to conduct at a particular measurement station in order to quantitatively and precisely estimate continuous fuel CO_2 within a measurement network.

2. The modelling framework

For the study's purpose of theoretically assessing precision and accuracy of different tracer configurations for fuel CO_2 estimation, it is only of secondary importance that modelled time series are correct, but it is mainly important that the model provides a reasonably realistic data set. In this study, we simulate mole fractions and isotopic records for the Heidelberg site (49°3' N, 8°4' E, urban, see Levin et al., 2003) and for two non-existing stations Gartow (53°0' N, 11°3' E, rural) and Berlin (52°5' N, 13°6' E, polluted) for the year 2012. All three stations may potentially be part of the German ICOS atmospheric network (see http://www.icos-infrastructure.eu/).

We used the Stochastic Time-Inverted Langrangian Transport (STILT) model (Lin et al., 2003) as well as pre-set source and sink distributions (see below). To simulate the atmospheric transport we used meteorological fields from the European Center for Medium-Range Weather Forecast with 3-hourly temporal resolution and 25 km x 25 km spatial resolution (Trusilova et al., 2010). Details of the STILT model are given in Lin et al. (2003) and in Gerbig et al. (2003); here we only provide a few relevant details. By emitting 100 particles (representing the observed air parcel) at the measurement location and time and inverting the meteorological fields in time, it is possible to follow the particles' trajectories backward in time using mean wind and a parameterization for the turbulent motion. For each of the trajectories, the sensitivity to emission fluxes is derived based on the residence time within the lower half of the mixed layer during each advection time step (typically 0.25 to 1 hours). The sensitivity of the observed tracer mole fraction to upstream emissions was derived by combining the sensitivities of each trajectory on a common horizontal grid (here 1/12° latitude x 1/8° longitude, corresponding to about 10 km x 10 km). To reduce impact from undersampling of upstream areas at times when particles are distributed over extensive areas with large gaps between neighboring particles, the effective horizontal size of the grid cells is increased dynamically with increasing separation of the particles (Gerbig et al., 2003). This allows efficient simulations with a relative small ensemble size. The sensitivity of the mole fraction at the measurement site to emissions located upstream is typically called footprint. The particles are traced back in time until they leave the model domain, which extends from 16°W to 36°E and from 32°N to 74°N. Initial/lateral CO_2 tracer boundary conditions for CO_2 tracer far-field mole fractions are taken from analyzed CO_2 fields, generated by the global atmospheric tracer transport model, TM3 (Heimann and Körner, 2003), based on optimized fluxes (Rödenbeck, 2005) transported at a spatial resolution of 4°× 5° with 19 vertical levels, and a temporal resolution of 6 hours (s96 v3.6, http://www.bgc-jena.mpg.de/~christian.roedenbeck/download-CO2-3D/). The footprint is multiplied with the biospheric and anthropogenic surface emissions to estimate the mole fraction change at the measurement site.

For the biospheric CO_2 fluxes, we use the vegetation photosynthesis and respiration model (VPRM, Mahadevan et al., 2008). The Net Ecosystem Exchange is calculated for different biome types based on SYNMAP (Jung et al., 2006) using land surface water index and enhanced vegetation index from MODIS (http://modis.gsfc.nasa.gov/) satellite data, as well as air temperature and short wave radiation from ECMWF. VPRM results are computed at 1/12° x 1/8° resolution with hourly resolution. We neglect biospheric CO and CH_4 fluxes in the model. CO destruction by OH and CO production via CH_4 oxidation is taken into account (Gerbig et al., 2003). However, CO production via non-methane hydrocarbon (NMHC) oxidation and CO uptake by soils (Conrad, 1996) are not included in the model. When using CO as tracer for fuel CO_2, neglecting natural CO sources and sinks may be problematic since natural sources would lead to an overestimation and natural sinks to an underestimation of fuel CO_2. We will discuss this in more detail in Sect. 3.3.2 and 3.4.

Anthropogenic emissions of CO_2, CO and CH_4 are from a preliminary version of the EDGARv4.3 emission inventory (EC-JRC/PBL, 2015), also used for the UNEP Emissions Gap Report (Rogelj et al., 2014) for the base year 2010 and have a spatial resolution of 0.1° x 0.1°. The emissions are further separated following IPCC emission categories, which are again separated in fuel types (i.e. hard coal, brown coal, oil, natural gas, derived gas, biofuels etc.). To extrapolate the emissions to the year 2012 specifically we follow the approach taken in the COFFEE dataset (CO_2 release and Oxygen uptake from Fossil Fuel Emission Estimate) (Steinbach et al., 2011) and use specific temporal factors (seasonal, weekly and daily cycles) (Denier van der Gon et al., 2011) for different emission categories, and apply country and fuel type specific year-to-year changes at national level taken from the BP statistical review of World Energy 2014 (available at: http://www.bp.com/en/global/corporate/about-bp/energy-economics/statistical-review-of-world-energy.html).

The STILT model calculates the total trace gas mole fraction of CO_2 (y_{tot}) at the measurement site as the sum of a background mole fraction y_{bg}, contributions from the biosphere y_{bio}, from different fossil fuel types $y_{ff,i}$ and different biofuel types $y_{bf,j}$:

$$y_{\mathrm{tot}} = y_{\mathrm{bg}} + y_{\mathrm{bio}} + \sum_{\mathrm{i}} y_{\mathrm{ff,i}} + \sum_{\mathrm{j}} y_{\mathrm{bf,j}} \tag{1}$$

The last two terms of Eq. (1) form the total fuel CO_2 (y_F). We can associate a total isotopic $\delta^{13}C(CO_2)$ (δ_{tot}) record to the total CO_2 record following Mook (2001):

$$\delta_{\mathrm{tot}} y_{\mathrm{tot}} \approx \delta_{\mathrm{bg}} y_{\mathrm{bg}} + \delta_{\mathrm{bio}} y_{\mathrm{bio}} + \sum_{\mathrm{i}} \delta_{\mathrm{ff,i}}\, y_{\mathrm{ff,i}} + \sum_{\mathrm{j}} \delta_{\mathrm{bf,j}}\, y_{\mathrm{bf,j}} \tag{2}$$

The isotopic signatures attributed to the different emission types, e.g. $\delta_{ff,i}$ and δ_{bio} are listed in Table 1. Note that we do not implement a diurnal cycle into the biospheric signature.

The total CO mole fraction (x_{tot}) can be balanced in analogy to CO_2, but we neglect biospheric CO contributions as they are expected to be small:

$$x_{\mathrm{tot}} = x'_{\mathrm{bg}} + \sum_i x_{\mathrm{ff,i}} + \sum_j x_{\mathrm{bf,j}} = x'_{\mathrm{bg}} + \sum_i \frac{y_{\mathrm{ff,i}}}{\overline{R_{\mathrm{ff,i}}}} + \sum_j \frac{y_{\mathrm{bf,j}}}{\overline{R_{\mathrm{bf,i}}}} \qquad (3)$$

The emission ratios $\overline{R_{\mathrm{ff,i}}}$ (=$\Delta x/\Delta y_{\mathrm{ff,i}}$) depend on the emission category as well as fuel type and are determined by the emission characteristics (implied emission factors) given in EDGARv4.3. The footprint-weighted mean ratios, e.g. $\overline{R_{\mathrm{F}}}$, are listed in Table A1 for Heidelberg. For the background values $\Delta^{14}C_{\mathrm{bg}}$, y_{bg}, δ_{bg} and x'_{bg} , we use those mole fractions where CH_4 mole fractions reach a minimum value within two days. This is mainly the case in the afternoon when vertical mixing is strongest (for more details on the choice of background see appendix A2). Note, that the CO background x'_{bg} is denoted with a prime, since it has been corrected for chemical reactions with OH (sink) and for production from oxidation of CH_4 by applying a first-order chemical reaction on hourly OH and CH_4 fields. The contributions of fossil fuel and biofuel CO, are, however, not corrected for these chemical reactions in the model, since the CO, which is released in the footprint area of the measurement site typically travels only a fraction of its actual life-time until arriving at the measurement site.

The $\Delta^{14}C(CO_2)$ ($\Delta^{14}C_{\mathrm{tot}}$) balance is also simulated and follows:

$$y_{\mathrm{tot}}(\Delta^{14}C_{\mathrm{tot}} + 1) \approx y_{\mathrm{bg}}(\Delta^{14}C_{\mathrm{bg}} + 1) + y_{\mathrm{bio}}(\Delta^{14}C_{\mathrm{bio}} + 1) + \sum_i y_{\mathrm{ff,i}}(\Delta^{14}C_{\mathrm{ff,i}} + 1) + \sum_j y_{\mathrm{bf,j}}(\Delta^{14}C_{\mathrm{bf,j}} + 1) \qquad (4)$$

With $\Delta^{14}C_{\mathrm{bio}}$, $\Delta^{14}C_{\mathrm{bf,j}}$ and $\Delta^{14}C_{\mathrm{ff,i}}$ listed in Table A1 and CO_2 mole fractions from model results. As all fossil fuel CO_2 sources are void of $^{14}C(CO_2)$, fuel CO_2 contributions are separated into fossil fuel and biofuel contributions.

In the following, we use six different tracers or tracer combinations to derive continuous fuel CO_2: CO_2-only, CO, CO as tracer for traffic and $\delta^{13}C$ as tracer for all fuel CO_2 except that of traffic, CO as tracer for biofuel CO_2 and $\delta^{13}C(CO_2)$ as tracer for fossil fuel CO_2, $\delta^{13}C(CO_2)$ and $\Delta^{14}C(CO_2)$. The six tracer combinations were qualitatively motivated and described in the introduction and the equations are derived in the appendix A1, are summarized in Table 2. They are briefly appointed here with their underlying assumptions: When using CO_2 as tracer for anthropogenic CO_2, we assume that all CO_2 stems from anthropogenic sources and no biospheric sources or sinks exist in the catchment area. In the CO-based method, we utilize that CO is co-emitted during anthropogenic CO_2 emissions and assume that we know the monthly mean ratio of y_F to x_F. In the $\delta^{13}C(CO_2)$ approach, we use the isotopic depletion of fuel CO_2 relative to biospheric CO_2 and assume to know the mean isotopic signature of fuel and biospheric CO_2. The $\Delta^{14}C(CO_2)$-based approach makes use of the fact that fossil fuel CO_2 contains no $^{14}C(CO_2)$ in contrary to biospheric (and biofuel) $\Delta^{14}C(CO_2)$. Both need to be known for calculation. We also investigate the combination of CO and $\delta^{13}C(CO_2)$, with CO as tracer for first, traffic CO_2 and second, biofuel CO_2 and $\delta^{13}C(CO_2)$ for the respective remaining fuel CO_2. This separation was made, since in Europe traffic and biofuel emissions both show a rather large ratio of CO/CO_2 compared to emissions from other sectors, which makes CO a suitable tracer for these sectors. When separating between traffic and non-traffic fuel CO_2, we need to know the monthly mean values for R_{tr}, m_{tr}, δ_{tr} and $\delta_{F\text{-}tr}$. This holds analogously for separation between fossil fuel and biofuel CO_2. The different targeted emission groups (fuel CO_2, fossil fuel CO_2, fuel CO_2 without traffic, traffic CO_2, biofuel CO_2 and biospheric CO_2) are also listed and characterized in Table A1.

3. Results

We investigated how well the different tracer combinations perform at a typical urban, rural and polluted measurement site. First, we will discuss the upper limit of precision and accuracy of fuel CO_2 estimation using these tracers when assuming all parameters (e.g. $\overline{\delta_F}$) are known at every time step. Here, the smallest possible time step is hours. We then investigate how the use of averaged accurate parameters and variables affects the fuel CO_2 estimate. Next, we also perform a sensitivity analysis to identify, which parameters and variables need to be known at which precision and accuracy for fuel CO_2 estimation with satisfying accuracy (of e.g. better than 10%). Finally, we discuss the diurnal variation of fuel CO_2 and include a realistic measurement uncertainty into our considerations.

3.1. High (hourly) resolution of parameters and variables

The integrated footprint-weighted parameters (e.g. $\overline{R_{\mathrm{F}}}$, $\overline{R_{\mathrm{tr}}}$, $\overline{R_{\mathrm{bf}}}$, $\overline{\delta_{\mathrm{F}}}$, $\overline{\delta_{\mathrm{ff}}}$, $\overline{\delta_{\mathrm{bf}}}$, $\overline{\delta_{\mathrm{tr}}}$, $\overline{\delta_{\mathrm{F-tr}}}$, $\overline{m_{\mathrm{bf}}}$ and $\overline{m_{\mathrm{tr}}}$) are needed for the estimation of fuel CO_2 using the tracers CO and $\delta^{13}C(CO_2)$ (see Appendix A1 for derivation and Table 2 for summary of all equations). These parameters are dependent on the emission characteristics of the sources in the catchment area of the measurement site. If e.g. the mean isotopic signature of fuel CO_2 sources in the catchment area varies or if the catchment area itself varies, the integrated footprint-weighted parameter $\overline{\delta_{\mathrm{F}}}$ will change. Typically, the integrated footprint-weighted parameters vary on time scales of hours, weeks, months and years. If, for a given measurement site, we could determine these parameters on the time scale of hours (which is the temporal resolution of our model), we would be able to estimate fuel CO_2 entirely correctly (difference of estimated and modelled fuel CO_2 would be zero) using CO and $\delta^{13}C(CO_2)$ or any combination of these tracers.

In contrast to methods using CO and/or $\delta^{13}C(CO_2)$, CO_2-only will overestimate fuel CO_2 when biospheric CO_2 contributions are positive (which will often be the case during night time and in winter) and underestimate fuel CO_2 when the biospheric CO_2 is negative (which may be the case during daytime in summer). This leads to time-dependent biases depending on the proportion of biospheric CO_2 to total CO_2 at the location, which is in general not negligible compared to the fuel CO_2 signal.

As $\Delta^{14}C(CO_2)$ is not sensitive to biofuel contributions, $\Delta^{14}C(CO_2)$ based fuel CO_2 estimates will underestimate the fuel CO_2 contributions approximately by the amount of biofuel CO_2 to the regional CO_2 concentration offset. Additionally, any $^{14}C(CO_2)$ emissions from nearby nuclear power plants or nuclear fuel reprocessing plants could potentially mask the depletion of fuel CO_2 contributions. Nuclear power plant emissions were not implemented in this model, but we will shortly discuss their possible effects in Sect. 5.

3.2. Low (monthly) resolution of parameters and variables

Normally it will not be possible to determine parameters such as $\overline{R_{\mathrm{F}}}$, $\overline{R_{\mathrm{F}}}$, $\overline{R_{\mathrm{tr}}}$, $\overline{R_{\mathrm{bf}}}$, $\overline{\delta_{\mathrm{F}}}$, $\overline{\delta_{\mathrm{ff}}}$, $\overline{\delta_{\mathrm{bf}}}$, $\overline{\delta_{\mathrm{tr}}}$, $\overline{\delta_{\mathrm{F-tr}}}$, $\overline{m_{\mathrm{bf}}}$ and $\overline{m_{\mathrm{tr}}}$ with hourly resolution. We, thus, investigate how using monthly median values of these parameters may influence the fuel CO_2 estimates. We will discuss later how we can obtain their monthly mean values and, for now, assume they are known on a monthly basis.

We now only use the monthly median value of the footprint-weighted parameters $\overline{R_{\mathrm{F}}}$, $\overline{R_{\mathrm{F}}}$, $\overline{R_{\mathrm{tr}}}$, $\overline{R_{\mathrm{bf}}}$, $\overline{\delta_{\mathrm{F}}}$, $\overline{\delta_{\mathrm{ff}}}$, $\overline{\delta_{\mathrm{bf}}}$, $\overline{\delta_{\mathrm{tr}}}$, $\overline{\delta_{\mathrm{F-tr}}}$, $\overline{m_{\mathrm{bf}}}$ and $\overline{m_{\mathrm{tr}}}$ to estimate fuel CO_2. Note, that we use the median instead of the mean value for the footprint-weighted parameters, since the median is less sensitive to outliers. Using only monthly median values will introduce sub-monthly inaccuracies into the fuel CO_2 estimate since the footprint-weighted parameters vary on sub-monthly timescales. The variability of the discrepancy between estimated and reference (directly modelled) fuel CO_2 estimates will depend on the magnitude of sub-monthly variations of $\overline{R_{\mathrm{F}}}$, $\overline{R_{\mathrm{F}}}$, $\overline{R_{\mathrm{tr}}}$, $\overline{R_{\mathrm{bf}}}$, $\overline{\delta_{\mathrm{F}}}$, $\overline{\delta_{\mathrm{ff}}}$, $\overline{\delta_{\mathrm{bf}}}$, $\overline{\delta_{\mathrm{tr}}}$, $\overline{\delta_{\mathrm{F-tr}}}$, $\overline{m_{\mathrm{bf}}}$ and $\overline{m_{\mathrm{tr}}}$, but also on their absolute values. For example, the more depleted the fuel CO_2 emissions are, the larger the isotopic difference between emissions from the biosphere and from fuel burning and the better the tracer $\delta^{13}C(CO_2)$ will be for fuel CO_2 emissions as both emission groups can be isotopically distinguished clearly (see Appendix C). For our model setting, the sub-monthly variations (standard deviation) are about ±3 (nmol/mol)/(µmol/mol) for $\overline{R_{\mathrm{F}}}$, $\overline{R_{\mathrm{tr}}}$ and $\overline{R_{\mathrm{bf}}}$, ± 0.2 (nmol/mol)/(nmol/mol) for $\overline{m_{\mathrm{bf}}}$ and $\overline{m_{\mathrm{tr}}}$, ±2 ‰ for $\overline{\delta_{\mathrm{F}}}$, $\overline{\delta_{\mathrm{ff}}}$, $\overline{\delta_{\mathrm{bf}}}$, $\overline{\delta_{\mathrm{tr}}}$ and $\overline{\delta_{\mathrm{F-tr}}}$ (variations due to varying footprints in the STILT model and temporal emission patterns of the different emission sectors). This variation is propagated into the fuel CO_2 estimate. The corresponding distribution of the difference between the estimated and modelled fuel CO_2 can be seen in Fig 1 for the station Heidelberg.

The mean difference between the modelled and tracer-based fuel CO_2 estimate provides a measure for the accuracy of the fuel CO_2 determination with the different tracer methods. In principle, one cannot assume that, when using the correct median values for $\overline{R_{\mathrm{F}}}$, $\overline{R_{\mathrm{F}}}$, $\overline{R_{\mathrm{tr}}}$, $\overline{R_{\mathrm{bf}}}$, $\overline{\delta_{\mathrm{F}}}$, $\overline{\delta_{\mathrm{ff}}}$, $\overline{\delta_{\mathrm{bf}}}$, $\overline{\delta_{\mathrm{tr}}}$ and $\overline{\delta_{\mathrm{F-tr}}}$ no median bias will be introduced into the CO_2 estimate. The reason is that the values for $\overline{R_{\mathrm{F}}}$, $\overline{R_{\mathrm{F}}}$, $\overline{R_{\mathrm{tr}}}$, $\overline{R_{\mathrm{bf}}}$, $\overline{\delta_{\mathrm{F}}}$, $\overline{\delta_{\mathrm{ff}}}$, $\overline{\delta_{\mathrm{bf}}}$, $\overline{\delta_{\mathrm{tr}}}$ and $\overline{\delta_{\mathrm{F-tr}}}$ are calculated on an hourly basis independent on the total fuel CO_2 value (y_F) at that time and are then averaged monthly. However, if y_F and $\overline{R_{\mathrm{F}}}$, $\overline{R_{\mathrm{tr}}}$, $\overline{R_{\mathrm{bf}}}$, $\overline{\delta_{\mathrm{F}}}$ $\overline{\delta_{\mathrm{ff}}}$, $\overline{\delta_{\mathrm{bf}}}$, $\overline{\delta_{\mathrm{tr}}}$ and $\overline{\delta_{\mathrm{F-tr}}}$ are correlated, sub-monthly over- and underestimation of y_F due to sub-monthly variation of $\overline{R_{\mathrm{F}}}$, $\overline{R_{\mathrm{F}}}$, $\overline{R_{\mathrm{tr}}}$, $\overline{R_{\mathrm{bf}}}$, $\overline{\delta_{\mathrm{F}}}$, $\overline{\delta_{\mathrm{ff}}}$, $\overline{\delta_{\mathrm{bf}}}$, $\overline{\delta_{\mathrm{tr}}}$ and $\overline{\delta_{\mathrm{F-tr}}}$ will not necessarily not average out. An analysis of the bias (difference between modelled and tracer-based CO_{2F} estimate; x-axis in Fig 1-3) introduced when using monthly median footprint-weighted parameters is therefore vital. The standard deviations of the Gaussian fits to the difference distributions (Fig 1-3) provide a measure for the precision of fuel CO_2 determination.

All methods using $\delta^{13}C(CO_2)$ and/or CO (Fig 1b-e, 2b-e and 3b-e) are able to estimate fuel CO_2 without significant systematic biases, if the annual median parameters $\overline{\delta_{\mathrm{ff}}}$, $\overline{\delta_{\mathrm{bf}}}$, $\overline{\delta_{\mathrm{tr}}}$, $\overline{\delta_{\mathrm{F-tr}}}$ and $\overline{R_{\mathrm{F}}}$ are known (see Sect. 3.3. for the case that they are not accurately known). Mean and median differences of modelled and estimated fuel CO_2 are within 10 % of the annual mean fuel CO_2 signal. The benefit when using CO additionally to $\delta^{13}C(CO_2)$ is very small, which is due to the fact that traffic or biofuel CO_2 contributions are not very distinct with respect to their isotopic signature or their CO/CO_2 emission ratio from the other fuel CO_2 contributions for our model settings. When using CO as tracer for fuel CO_2 (Fig 1b, 2b and 3b) the standard deviation of the difference between the estimated and the true fuel CO_2 value is larger than when using $\delta^{13}C(CO_2)$. The reason is the large sub-monthly variation of footprint-weighted $\overline{R_{\mathrm{F}}}$ in our modelled data.

Generally, the absolute standard deviation of the different tracer distributions is larger at the polluted station than at urban and rural stations. At the same time, we found that the variation of the footprint-weighted parameters such as $\overline{R_{\mathrm{F}}}$, $\overline{R_{\mathrm{F}}}$, $\overline{R_{\mathrm{tr}}}$, $\overline{R_{\mathrm{bf}}}$, $\overline{\delta_{\mathrm{F}}}$, $\overline{\delta_{\mathrm{ff}}}$, $\overline{\delta_{\mathrm{bf}}}$, $\overline{\delta_{\mathrm{tr}}}$, $\overline{\delta_{\mathrm{F-tr}}}$, $\overline{m_{\mathrm{bf}}}$ and $\overline{m_{\mathrm{tr}}}$ is largest in rural areas and smallest in polluted areas, which is probably due to the fact that in polluted catchment areas the many polluters homogenize partly, whereas at cleaner sites the emissions of the few different polluters are temporally and spatially distinct. Hence, the larger spread of the fuel CO_2 estimate at polluted stations is not the result of larger source heterogeneity, but is due to the larger absolute signals (and with that larger absolute variations) of fuel CO_2 in the catchment area of these sites. Only CO_2 as tracer for fuel CO_2 shows less variability at the polluted site Berlin, which is due to smaller contribution from the biosphere in its catchment area. However, the relative variability ($=1\sigma/\mathrm{mean}(y_F)$) is significantly higher in Gartow (e.g. $\delta^{13}C$-method: 20 %) than it is in Heidelberg or Berlin (both ca. 5%). Differences and spreads of the CO_2-only and $^{14}C(CO_2)$ method were already described in Sect. 3.1.

We have found that only small median differences occur when using $\delta^{13}C(CO_2)$ or CO as tracer for fuel CO_2. This finding is only valid under the premise, that the median values of all input and footprint-weighted parameters are known. If one or more of the parameters or variables are assigned incorrectly, this will lead to a systematic error of the fuel CO_2 estimate. The sensitivity of this misassignment for the different parameters and variables will be assessed in the next chapter.

3.3. Sensitivity of fuel CO_2 estimates on misassigned parameters and variables

We have investigated how well we are able to estimate fuel CO_2 in a setting in which e.g. the monthly averages of all parameters are perfectly well known, but temporally varying on shorter time scale. However, since, in reality, parameters such as $\overline{\delta_{\mathrm{F}}}$ or $\overline{R_{\mathrm{F}}}$ are only approximately known, we need to investigate how a misassignment of one of these parameters will influence fuel CO_2 estimates. This will provide information on how well certain parameters and variables need to be assigned for a fuel CO_2 estimate with targeted accuracy. For this purpose, we misassign one parameter and, at the same time, keep the other parameters at their correct value. We then determine how the fuel CO_2 estimate changes (y-axis in Fig 4) when the misassignment of the parameter (x-axis) varies. The sensitivities of all methods to the most important parameters and variables are shown in Figure 4 exemplary for the urban site Heidelberg. We have done this analysis for the parameters $CO_{2\mathrm{tot}}$ (Fig 4a), $\delta^{13}C_{\mathrm{tot}}$ (Fig 4b), $CO_{2\mathrm{bg}}$ (Fig 4c), $\delta^{13}C_{\mathrm{bg}}$ (Fig 4d), $\overline{\delta_{\mathrm{F}}}$ (Fig 4e), $\overline{\delta_{\mathrm{bio}}}$ (Fig 4f), $\overline{\delta_{\mathrm{bf}}}$ (Fig 4g), $\overline{\delta_{\mathrm{tr}}}$ (Fig 4h), CO offset (Fig 4i), $\overline{m_{\mathrm{bf}}}$, $\overline{m_{\mathrm{tr}}}$ (Fig 4j), $\overline{R_{\mathrm{tr}},\ R_{\mathrm{bf}}}$ (Fig 4k), $\overline{R_{\mathrm{F}}}$ (Fig 4l), $\Delta^{14}C_{\mathrm{tot}}$ (Fig 4m) , $\Delta^{14}C_{\mathrm{bg}}$ (Fig 4n), $\Delta^{14}C_{\mathrm{bio}}$ (Fig 4o) and $\Delta^{14}C_{\mathrm{bf}}$ (Fig 4p). The variation of these values was chosen in a way that the range includes the typical measurement precision for $CO_{2\mathrm{meas}}$, $CO_{2\mathrm{bg}}$, δ_{bg}, δ_{meas}, $\Delta^{14}C_{\mathrm{bg}}$ and $\Delta^{14}C_{\mathrm{meas}}$. The variation of the CO offset was chosen in a way that it displays the measurement precision of total CO and of the background CO, but also includes realistic contributions from natural CO sources and sinks. For the parameters$\overline{R_{\mathrm{F}}}$, $\overline{R_{\mathrm{F}}}$, $\overline{R_{\mathrm{tr}}}$, $\overline{R_{\mathrm{bf}}}$, $\overline{\delta_{\mathrm{F}}}$, $\overline{\delta_{\mathrm{ff}}}$, $\overline{\delta_{\mathrm{bf}}}$, $\overline{\delta_{\mathrm{tr}}}$, $\overline{\delta_{\mathrm{F-tr}}}$, $\overline{m_{\mathrm{bf}}}$, $\overline{m_{\mathrm{tr}}}$, $\Delta^{14}C_{\mathrm{bio}}$ and $\Delta^{14}C_{\mathrm{bf}}$, we selected realistic ranges of sub-monthly parameter variation.

The error bars given on the right hand side of Figure 4 show the interquartile ranges (IQR) and stem from the sub-monthly variability of $\overline{\delta_{\mathrm{F}}}$, $\overline{R_{\mathrm{F}}}$, $\overline{m_{\mathrm{bf}}}$ and $\overline{\mathrm{m}_{\mathrm{tr}}}$, which was discussed in chapter 3.2. One can directly identify critical parameters and variables, for which the difference between the modelled and estimated fuel CO_2 (y-axis) changes significantly with increasing misassignment of parameters/variables (x-axis).

3.3.1 Sensitivity of CO_2-only method

We confirm that the CO_2–only method (green in Fig 4) is insensitive to the variation of the displayed parameters/variables.

3.3.2 Sensitivity of CO method

Critical parameters/variables of the CO method (orange in Fig 4) are the CO offset ΔCO (Fig 4i), as well as the ratio $\overline{R_F}$ (=$\Delta x/y_F$) (Fig 4l). In practise, the CO offset is derived by subtracting the CO background as well as natural CO source and sink contributions from the total measured CO mole fraction. Typical fuel CO offsets are in the order of 40 nmol/mol. In our model we have not included natural CO sources and sinks, but in practise, the uncertainty of the CO mole fraction measurement and of the natural CO contributions will add to the uncertainty of the fuel CO_2 estimate. Assuming e.g. a CO background, which is 15 nmol/mol too large, or assuming an additional sink resulting in a 15 nmol/mol lower CO background, which may be a realistic diurnal variation of natural CO variation (Gros et al., 2002; Vogel, 2010), would lead to a significant overestimation of fuel CO_2 of about 2.5 μmol/mol (median). Therefore, for a real data set, it is vital to determine the natural CO contributions and sinks (also soil sinks) using chemistry models or calibration with e.g. $\Delta^{14}C(CO_2)$ (see Sect. 4). In Heidelberg, the median modelled ratio $\overline{R_F}$ is about 5 (μmol/mol)/(nmol/mol) and shows a rather large variation of 3 (nmol/mol)/(μmol/mol). Fig. 4l shows, that such a variation of $\overline{R_F}$ contributes significantly to the imprecision of fuel CO_2 in the CO-method. Also, the correct determination of $\overline{R_F}$ is vital for accurate fuel CO_2 estimates using CO.

3.3.3 Sensitivity of methods using $\delta^{13}C(CO_2)$

The sensitivities of fuel CO_2 estimates using $\delta^{13}C(CO_2)$ only (blue in Fig 4) and combinations of $\delta^{13}C(CO_2)$ and CO are rather similar (red and black in Fig 4). Note that the sensitivity on δ_{bg} or δ_{tot} is plotted when keeping y_{bg} and y_{tot} constant. Changing the y_{bg} or y_{tot} values at the same time when changing δ_{bg} or δ_{tot} (following a Keeling curve (Keeling, 1958; 1960) with typical mean $\delta^{13}C$ source of -25 ‰) results in about a factor ten smaller sensitivity and is therefore not critical. However, small $\delta^{13}C(CO_2)$ variations (e.g. due to finite measurement precision or small inaccuracies), which are uncorrelated with CO_{2tot}, lead to large biases in fuel CO_2, e.g. a measurement bias of δ_{tot}=0.1 ‰ leads to a fuel CO_2 misassignment of 5 (μmol/mol) (see Fig 4b). Therefore, a high measurement precision as well as accuracy of $\delta^{13}C(CO_2)$ is required for precise and accurate fuel CO_2 estimation. Further critical parameters of the methods using $\delta^{13}C(CO_2)$ are the isotopic signature of fuel CO_2 and the isotopic signature of biospheric CO_2 in the footprint (see Fig 4e, f). The isotopic signatures of fuel and biospheric CO_2 must therefore be well known (or potentially calibrated, see Sect. 4), if we want to use $\delta^{13}C(CO_2)$ as tracer for fuel CO_2. Especially assuming more enriched fuel isotopic signatures or too depleted biospheric signatures biases the fuel CO_2 estimates strongly, because in these cases, biospheric and fuel CO_2 sources are difficult to distinguish using $\delta^{13}C(CO_2)$.

3.3.4 Sensitivity of $\Delta^{14}C(CO_2)$*method*

Figures 4 m-p display the sensitivity of the $\Delta^{14}C(CO_2)$ based estimate of fuel CO_2 on the variables $\Delta^{14}C_{tot}$, $\Delta^{14}C_{bg}$ and $\Delta^{14}C_{bio}$. While fuel CO_2 is rather insensitive against misassignment of $\Delta^{14}C(CO_2)_{bio}$ (Fig 4o) and $\Delta^{14}C(CO_2)_{bf}$ (Fig 4p), it is very sensitive on $\Delta^{14}C(CO_2)_{tot}$ (Fig 4m) and $\Delta^{14}C(CO_2)_{bg}$ (Fig 4n) as was already described in Turnbull et al. (2007). Thus, precise and accurate $\Delta^{14}C(CO_2)$ measurements are important for fuel CO_2 determination. Note, that the best currently achieved measurement precision of conventional counting or AMS measurements is ± 2‰ (equivalent to about ±1.0 μmol/mol fuel CO_2), but the hypothetical future continuous GC-AMS measurements may be of order ± 5‰ (equivalent to about ± 3 μmol/molfuel CO_2). The reason why the fuel (biofuel + fossil fuel) CO_2 estimate based on ^{14}C is biased by about 1.1 μmol/mol is due to the fact that biofuel CO_2, in contrast to fossil fuel CO_2, contains $^{14}C(CO_2)$ and is therefore not detectable by lack of $^{14}C(CO_2)$.

3.4 Measurement precision and sub-monthly variation of parameters/variables

In Sect. 3.3.1-3.3.4, we have seen how sensitive the fuel CO_2 estimates are to the total mole fractions and *δ/Δ*–values. Since they have a large impact on the fuel CO_2 estimate, we now include their uncertainty into our analysis of precision of fuel CO_2 estimation. In order to display the effect of a limited measurement precision of CO_2, CO, $\delta^{13}C(CO_2)$ and $\Delta^{14}C(CO_2)$ we construct random realizations with mean value zero and a specific standard deviation. Additionally, we add a random variation to the CO offset and the biospheric/biofuel isotopic (*δ/Δ*-) signature in order to simulate the effect of variability of CO to CO_2 ratio and of isotopic end members. These random uncertainties were not included in Sec 3.1 and 3.2 and in Fig 1-3. Note, that in reality these variations may not be randomly distributed. E.g. we may introduce a systematic bias in one direction if we have unaccounted production of CO from VOCs or, if we have unaccounted CO (e.g. soil) sinks. These sources and sinks will not occur randomly, but have a distinct sub-monthly pattern. Depending on the sign of the net natural CO flux, the bias may be positive or negative. However, for simplicity, we also include the natural CO variation here as a random vector as no natural CO sinks or sources are included in the modelled CO offset, but we want to show the possible effect of their variation.

The random vectors, which were used in this study are summarized in Table 3 with their magnitude being motivated. The distributions of the difference between estimated (incl. measurement and parameter uncertainties and sub-monthly variations) and modelled fuel CO_2 can be seen in Fig 5-7. Note that a possible misassignment of parameters or variables as investigated in Fig 4 is neither accounted for in Fig 1-3 nor in Fig 5-7.

When including the measurement uncertainties and (input and footprint-weighted) parameter variability into the considerations, the mean bias remains unaltered, since the included uncertainty is random. However, the distributions of the CO and $\delta^{13}C(CO_2)$-based approaches for rural sites (such as Gartow), medium polluted sites (such as Heidelberg) and polluted sites (such as Berlin) widen significantly by about the same amount for all three sites. This is due to identical assumed measurement precisions and parameter variations. Since the absolute fuel CO_2 offset is larger in Berlin (annual modelled average ca. 25 µmol/mol), than in Heidelberg (16 µmol/mol), and in Gartow (3 µmol/mol), the relative variability ($=1\sigma/\mathrm{mean}(y_F)$) is smallest for the measurement site in Berlin (e.g. ca. 15 % for $\delta^{13}C(CO_2)$-method) and largest for Gartow (110 % for $\delta^{13}C(CO_2)$-method). At present, it is therefore questionable whether the estimation of continuous fuel CO_2 is at rural measurement sites. Even $\Delta^{14}C(CO_2)$ measurements with a precision of 5 ‰ result in a variability in fuel CO_2 of 60%, but a $\Delta^{14}C(CO_2)$ precision of 2 ‰ would lead to a variability in fuel CO_2 of only 35% at rural sites (not shown here). The reduced precision of fuel CO_2 estimates, which we observe when including limited measurement precision into our considerations, highlights again the necessity of performing precise atmospheric measurements of $\delta^{13}C(CO_2)$ and CO_2 if we want to use $\delta^{13}C(CO_2)$ as tracer for fuel CO_2.

For urban sites, CO and $\delta^{13}C(CO_2)$-based methods show a very similar precision of about 4 µmol/mol (1σ). At urban sites, $\delta^{13}C(CO_2)$ is slightly more precise than CO. It is worth pointing out that CO_2-only may be an adequate tracer for fuel CO_2 in polluted areas in the winter time as absolute biases are small (<4%) and the precision (ca. 12 %) is rather good. $\Delta^{14}C(CO_2)$

measurements with a precision of 5 ‰ would be the best tracer at all stations, but is currently not available yet.

3.5. Comparison of the estimated fuel CO_2 diurnal cycle with different tracer configurations

As the diurnal cycle of CO_2 emissions is coupled to a diurnal change of the atmospheric mixing layer height, CO_{2F} mole fraction varies during the day. In our calculations, we only use monthly median values of $\overline{R_{\mathrm{F}}}$, $\overline{R_{\mathrm{F}}}$, $\overline{R_{\mathrm{tr}}}$, $\overline{R_{\mathrm{bf}}}$, $\overline{\delta_{\mathrm{F}}}$, $\overline{\delta_{\mathrm{ff}}}$, $\overline{\delta_{\mathrm{bf}}}$, $\overline{\delta_{\mathrm{tr}}}$, $\overline{\delta_{\mathrm{F-tr}}}$, $\overline{m_{\mathrm{bf}}}$ and $\overline{m_{\mathrm{tr}}}$ for CO_{2F} estimation. Discrepancies between the modelled reference diurnal cycle and the tracer based diurnal cycle may be introduced due to a diurnal cycle of the parameters $\overline{R_{\mathrm{F}}}$, $\overline{R_{\mathrm{F}}}$, $\overline{R_{\mathrm{tr}}}$, $\overline{R_{\mathrm{bf}}}$, $\overline{\delta_{\mathrm{F}}}$, $\overline{\delta_{\mathrm{ff}}}$, $\overline{\delta_{\mathrm{bf}}}$, $\overline{\delta_{\mathrm{tr}}}$, $\overline{\delta_{\mathrm{F-tr}}}$, $\overline{m_{\mathrm{bf}}}$ and $\overline{m_{\mathrm{tr}}}$. We thus need to test if we are able to reproduce the diurnal fuel CO_2 pattern in order to estimate fuel CO_2 from tracers at sub-diurnal resolution. Therefore, we calculate the median diurnal CO_{2F} cycles with the different methods and compare them to the reference model diurnal cycle for summer and for winter (see Fig 8 exemplary for the urban station Heidelberg).

One can see that the $\delta^{13}C(CO_2)$ method reproduces the reference diurnal cycle within its variability very well (standard errors of the respective hour in a half year are denoted as error bars in Fig 8). Median hourly differences are about 0.1 ± 0.7 µmol/mol for methods using $\delta^{13}C(CO_2)$. The CO_2-only method largely overestimates fuel CO_2 contributions during the night by up to 10 µmol/mol in winter and by about 15-25 µmol/mol in summer. During the afternoon, the CO_2–only method overestimates fuel CO_2 in winter and underestimates it in summer. Even though the absolute difference is small during the afternoon, the relative difference is still large. The CO_2–only method is therefore not able to trace the diurnal fuel CO_2 variation at a site like Heidelberg correctly. Using $\Delta^{14}C(CO_2)$ for fuel CO_2 estimation leads to a slight median underestimation throughout the day (and season), which is due to the presence of $^{14}C(CO_2)$ in biofuel CO_2 masking all biofuel CO_2 contributions. The CO-method slightly overestimates fuel CO_2 during nighttime by about 10% in winter and 20 % in summer. The standard deviation of the hourly medians of the differences between model and CO-based fuel CO_2 is about 15 % of the total fuel CO_2.

One could consider implementing a diurnal correction into the fuel CO_2 estimate in a way that not only monthly median values of $\overline{R_{\mathrm{F}}}$, $\overline{R_{\mathrm{tr}}}$, $\overline{R_{\mathrm{bf}}}$, $\overline{\delta_{\mathrm{F}}}$ $\overline{\delta_{\mathrm{ff}}}$, $\overline{\delta_{\mathrm{bf}}}$, $\overline{\delta_{\mathrm{tr}}}$, $\overline{\delta_{\mathrm{bio}}}$, $\overline{\delta_{\mathrm{F-tr}}}$, $\overline{m_{\mathrm{bf}}}$ and $\overline{m_{\mathrm{tr}}}$ are used, but also hourly correction factors for these parameters are multiplied (c.f. Vogel et al. 2010). This will be advantageous if the parameters exhibit a significant diurnal cycle themselves. However, for our setting, implementing a diurnal correction factor only slightly improves the agreement between the model and the estimated fuel CO_2 (not shown here). The reason is that the (hourly) median footprint-weighted parameters do not influence the (hourly) median fuel CO_2 estimates linearly, and that the synoptic variations of the footprint-weighted parameters are larger than the diurnal variations. Therefore, an hourly median correction factor does not necessarily improve the hourly fuel CO_2 estimate. We note that no diurnal systematic variability of the isotopic biospheric (respiration and photosynthesis) signature as well as of the non fuel CO sinks and sources (which would be treated as an enhancement or reduction of the CO offset ΔCO) were implemented, but only random uncertainties of ± 2 ‰ for δ_{bio} and ± 15 nmol/mol for ΔCO. This assumption of random variability will not be correct, if systematic (e.g. diurnal) variation of $\delta^{13}C_{\mathrm{bio}}$ and non fossil ΔCO variation occur. For $\delta^{13}C_{\mathrm{bio}}$ the diurnal changes are expected to be small (<1 ‰ (Flanagan et al., 2005) corresponding to CO_{2F} biases of <0.5 μmol/mol), but for CO these may be larger (e.g. diurnal natural ΔCO variation of about 10 nmol/mol may occur from dry deposition of CO in forest soils during night and from photochemical production of CO by hydrocarbons during the day (Gros et al., 2002) corresponding to ca. 2.5 μmol/mol fuel CO_2). Therefore, in a real setting, it might be necessary to model natural CO concentration in order to not introduce a bias into diurnal y_{F} structures.

In inverse model studies, often only afternoon hours are used to derive fluxes, as the atmospheric mixing can be better simulated by the models during conditions with a well developed mixed layer (Gerbig et al., 2008). Therefore, it is especially important to check the afternoon values of CO_{2F}. Figure 8 shows an enlarged inlay of the diurnal cycle during the afternoon hours. Since in this model study we use the minimum of total CH_4 values within two days as background value (Appendix A2), the afternoon offsets are very small, leading to a low signal to noise ratio. However, differences between the $\delta^{13}C(CO_2)$, CO, and $\Delta^{14}C(CO_2)$-based and reference fuel CO_2 are very small as well (mean differences <10 % of afternoon fuel CO_2 value, standard deviation of differences about 30%). Therefore, it seems justified to use an ensemble of afternoon values of continuous fuel CO_2 estimates (based on δ^{13}C(CO_2) or CO) for inverse model studies despite the small absolute fuel CO_2 values of about 1-2 µmol/mol in the afternoon hours at an urban site.

4. Calibration of $\overline{\delta_{\mathrm{F}}}$, $\overline{\delta_{\mathrm{F-tr}}}$, $\overline{\delta_{\mathrm{ff}}}$ and $\overline{R_{\mathrm{F}}}$ with Δ^{14}C(CO_2) measurements

In order to estimate fuel CO_2 accurately with methods using CO and/or δ^{13}C(CO_2), the parameters $\overline{\delta_{\mathrm{F}}}$, $\overline{\delta_{\mathrm{F-tr}}}$, $\overline{\delta_{\mathrm{ff}}}$ (and δ_{bio}) and $\overline{R_{\mathrm{F}}}$ need to be known with high accuracy, since otherwise biases are introduced into the fuel CO_2 estimate (see Fig 4). However, for the evaluation of a measured data set, $\overline{\delta_{\mathrm{F}}}$, $\overline{\delta_{\mathrm{F-tr}}}$, $\overline{\delta_{\mathrm{ff}}}$, δ_{bio} and $\overline{R_{\mathrm{F}}}$ are not per se available, but require either extensive source sampling campaigns or good bottom-up inventories. Alternatively, these parameters could also be “calibrated” using fossil fuel CO_2 estimates from Δ^{14}C(CO_2) measurements with high precision (in addition to biofuel contributions, which need to be added on top). For this purpose, Eq. (1) and (2) can be re-arranged and solved for calibration of $\overline{\delta_{\mathrm{F}}}$, $\overline{\delta_{\mathrm{F-tr}}}$, $\overline{\delta_{\mathrm{ff}}}$ or $\overline{R_{\mathrm{F}}}$ (for derivation see Appendix B).

Since Δ^{14}C(CO_2) measurements are time-consuming and costly, in practice only a limited number of Δ^{14}C(CO_2) measurements can be regulary performed. For example, in the Integrated Carbon Observation System (ICOS) atmospheric network, the radiocarbon measurement capacity was designed for about 50 radiocarbon measurements per station per year of which about 26 will be used for integrated sampling for long-term monitoring of fossil fuel CO_2.

Previous radiocarbon calibration approaches suggested integrated (e.g. monthly) sampling of Δ^{14}C(CO_2) for CO tracer calibration (cf. Levin and Karstens (2007) and Vogel et al., (2010) for $\overline{R_{\mathrm{F}}}$). Another possible approach for tracer calibration is to take grab samples rather than integrated samples (e.g. Turnbull et al., 2011). Grab samples could be taken through-out the year and the derived parameters $\overline{R_{\mathrm{F}}}$ and $\overline{\delta_{\mathrm{F}}}$, $\overline{\delta_{\mathrm{F-tr}}}$, $\overline{\delta_{\mathrm{ff}}}$ could then be averaged to one median value or separated into seasons and averaged to separate values e.g. for summer and winter. The optimal sampling strategy depends on the structure, variation and noise of $\overline{R_{\mathrm{F}}}$ and $\overline{\delta_{\mathrm{F}}}$, $\overline{\delta_{\mathrm{F-tr}}}$, $\overline{\delta_{\mathrm{ff}}}$ within one year. Principally, it would also be possible to take all the samples consecutively at 2 hour intervals during a so-called “event” and calculate the median value from the event. Therefore, we compare here four different sampling strategies for parameter calibration, all using a total of n samples per year (in ICOS: n≈24). Note that we include sub-monthly variation into the parameters and measurement uncertainties into the observations (as in Sect 3.4).

1. Integrated sample calibration: Take n/24 integrated samples each month and their associated background samples (for n≈24 that makes 12 monthly samples and 12 monthly background samples a year) and calibrate $\overline{R_{\mathrm{F}}}$ and $\overline{\delta_{\mathrm{F}}}, \overline{\delta_{\mathrm{F-tr}}}, \overline{\delta_{\mathrm{ff}}}$ on a monthly basis from the integrated samples (this corresponds to the approach suggested by Levin and Karstens (2007) and Vogel et al., (2010) for $\overline{R_{\mathrm{F}}}$). In this approach, the mean ΔCO and fuel ΔCO_2 (from integrated CO and $\Delta^{14}C(CO_2)$ sampling) over the course of one month are used to calculate monthly $\frac{\langle\Delta x\rangle}{\langle\Delta y\mathrm{F}\rangle}$. However, since actually the mean of ratio $\overline{R_{\mathrm{F}}}$ $=\langle\frac{\Delta x}{\Delta y\mathrm{F}}\rangle$ is required, and not the ratio of means $\frac{\langle\Delta x\rangle}{\langle\Delta y\mathrm{F}\rangle}$ (Vogel et al., 2010), biases may be introduced into the CO_{2F} estimate (same holds for the factors in $\overline{\delta_{\mathrm{F}}}$, $\overline{\delta_{\mathrm{F-tr}}}$ and $\overline{\delta_{\mathrm{ff}}}$).

2. Annual grab sample calibration: Randomly select a number of samples n/2 (and their associated afternoon background (n/2)) each year and calibrate annual median $\overline{R_{\mathrm{F}}}$ and $\overline{\delta_{\mathrm{F}}}, \overline{\delta_{\mathrm{F-tr}}}, \overline{\delta_{\mathrm{ff}}}$. Biases introduced by this sampling strategy are twofold; first, the random choice of grab samples may not represent the median annual value. This potential bias decreases with increasing number of grab samples used. Second, the potential seasonal cycle of the parameters is not considered. Therefore, in the annual grab sample calibration, the winter-time and summer-time fuel CO_2 estimates will always be shifted against each other, if $\overline{R_{\mathrm{F}}}$ and $\overline{\delta_{\mathrm{F}}}, \overline{\delta_{\mathrm{F-tr}}}, \overline{\delta_{\mathrm{ff}}}$ exhibit a seasonal cycle, but only one annual median value for these parameters would be used.

3. Seasonal grab sample calibration: Randomly select a number of samples n/4 (and their associated afternoon background (n/4)) in summer and in winter and calibrate a median $\overline{R_{\mathrm{F}}}$ and $\overline{\delta_{\mathrm{F}}}, \overline{\delta_{\mathrm{F-tr}}}, \overline{\delta_{\mathrm{ff}}}$ with half-yearly resolution. Here again, the random choice of grab samples may not represent the median half annual value, and a potential bias may be even larger here than in the annual grab sample calibration, since only half the samples are available to obtain a robust value for $\overline{R_{\mathrm{F}}}$ and $\overline{\delta_{\mathrm{F}}}, \overline{\delta_{\mathrm{F-tr}}}, \overline{\delta_{\mathrm{ff}}}$ for summer and winter.

In return, it is principally possible to detect the seasonal variation of $\overline{R_{\mathrm{F}}}$ and $\overline{\delta_{\mathrm{F}}}, \overline{\delta_{\mathrm{F-tr}}}, \overline{\delta_{\mathrm{ff}}}$.

4. Seasonal event calibration: Randomly select an "event day" each season. On this day, select n/2-2 consecutive grab samples (and 1 associated afternoon background) and calibrate a median $\overline{R_{\mathrm{F}}}$ and $\overline{\delta_{\mathrm{F}}}, \overline{\delta_{\mathrm{F-tr}}}, \overline{\delta_{\mathrm{ff}}}$ with half-yearly resolution. This approach is similar to approach 3, but entails a greater risk of choosing an event, which is not representative for the entire season, since subsequent samples are not independent of each other. On the other hand, it has the advantage of using more calibrations for the same number of radiocarbon measurements as approach 3 since only one background sample is needed for each event. However, if the background sample is biased, it will influence the entire event.

Comparing these sampling strategies to each other using one model run is difficult, since the result changes from random realization to random realization, depending on the selection of calibration samples in sampling strategy 2-4. We have therefore performed a Monte-Carlo simulation (with 500 runs) and used the root median square difference between the obtained and originally modelled reference values $\overline{R_{\mathrm{F}}}$ and $\overline{\delta_{\mathrm{F}}}, \overline{\delta_{\mathrm{F-tr}}}, \overline{\delta_{\mathrm{ff}}}$ to calculate the difference between tracer-based estimate and modelled reference fuel CO_2.

Table 4 shows the mean difference and standard deviation (as determined from a Gaussian fit to the difference histogram of modelled and tracer-based fuel CO_2, in analogy to Fig 5) for an urban setting. One can see that the "integrated sample calibration" causes biases due to the covariance of the factors in Eq. (B1) - (B4). The effect is much stronger for methods using δ^{13}C (ca. 15 % of mean fuel CO_2 offset in Heidelberg (16 µmol/mol) than for the CO method (ca. 5 %). This bias is directed meaning that it is not a random uncertainty, but actually a systematic bias introduced by computation. This is different from the calibrations on grab samples, which have a bidirectional absolute difference. Bidirectional differences may be advantageous over unidirectional differences when analyzing long-term records as bi-directional differences contribute to long-term noise rather than biases. For CO, it seems that the integrated calibration approach works well, but a uni-directed bias remains. Note, that the differences found here are not due to the insensitivity of biofuel CO_2

contributions of $\Delta^{14}C(CO_2)$, as we add the (assumed as known) biofuel CO_2 prior to “calibration” (see Eq. (B1)-(B3)).

We further find that since $\overline{\delta_{\mathrm{F}}}$, $\overline{\delta_{\mathrm{F-t}r}}$ $\overline{\delta_{\mathrm{ff}}}$ and $\overline{R_{\mathrm{F}}}$ do not exhibit a strong annual cycle, but show rather large, high-frequent variations, the best sampling strategy for 24 available radiocarbon measurements per year (as would be the case for the ICOS network) is using all available samples to calibrate well-defined median annual values of $\overline{R_{\mathrm{F}}}$ and $\overline{\delta_{\mathrm{F}}}$, $\overline{\delta_{\mathrm{F-tr}}}$, $\overline{\delta_{\mathrm{ff}}}$ (sampling strategy 2). Only, with 96 (or more) available radiocarbon measurements, it may be advisable to group the calibrations into half-yearly intervals. Having such many radiocarbon grab samples available may be a realistic scenario, if the parameters do not show any trend over the course of several years. Note, that a monthly grab sample calibration (not shown here) results in large biases of about ±3 μmol/mol for CO-based as well as $\delta^{13}C(CO_2)$-based methods and are thus, not advisable.

The accuracy of the seasonal event calibration is slightly worse than the accuracy of the seasonal calibration (see Table 4) due to non-representativeness of a single event for the entire season.

5. Discussion and Conclusion

In this work, we analyzed the advantages and disadvantages of different tracers for estimating continuous fuel CO_2 at different types of measurement stations. The accuracy and precision of continuous fuel CO_2 estimates at three exemplary stations, one rural, one urban and one polluted site were calculated. This should serve as orientation for the development of an atmospheric measurement strategy, so that the best tracer configuration for a particular station can be chosen to resolve the different CO_2 source components over a country or region. The results can be used to plan and construct new measurement networks and sampling strategies with the goal of deriving fuel CO_2 concentrations at high temporal resolution.

The results of our model study suggest that with our current measurement precision of continuous tracers such as CO, $\delta^{13}C(CO_2)$ (or $\Delta^{14}C(CO_2)$), in general it is not possible to estimate fuel CO_2 at rural areas (5 μmol/mol or less of CO_{2F}) with a precision better than 100% (due to the small signal to noise ratio. It could still be possible to monitor single pollution events since the signal to noise ratio is much higher during such events. At present, it thus seems not helpful to equip measurement stations in rural areas with continuous $\delta^{13}C(CO_2)$ and CO measurements with the objective of monitoring continuous fuel CO_2. However, it seems that tracer-based CO_{2F} monitoring may be possible at urban or polluted sites (as e.g. planned within the Megacities Carbon project) and may have the potential to improve the fuel CO_2 bottom-up inventories.

We find that CO_2-only cannot be used as tracer for fuel CO_2, as a significant contribution of CO_2 is released or taken up by the biosphere even in winter time. Only during winter in strongly polluted areas, biogenic CO_2 contributions lead to a relatively small bias of about 5% with the CO_2-only approach and asmall variation (σ/mean(y_F): 5%, see Fig 7).

In contrary to CO_2-only, CO and $\delta^{13}C(CO_2)$ can be used as tracer for fuel CO_2 in summer and in winter at urban and polluted sites. The accuracy of CO- and/or $\delta^{13}C(CO_2)$-based fuel CO_2 estimates depends to a large degree on how well the different parameters such as e.g. $\overline{R_F}$, $\overline{\delta_F}$, and δ_{bio} are known. Missasignment leads to significant biases in the fuel CO_2 estimate (Fig 4). Therefore, in practice, it is important to screen and monitor all sources and sinks in the catchment area of the measurement site and to determine the median isotopic source signature and the median ratios $\overline{R_F}$, $\overline{R_{tr}}$, $\overline{R_{bf}}$ as well as the CO offset as accurately as possible, e.g. by calibration with co-located $\Delta^{14}C(CO_2)$ measurements. The accuracy of the CO_{2F} estimate after ^{14}C-calibration depends strongly on the number of radiocarbon samples available for calibration and on the sampling strategy used. E.g. In the ICOS project, approximately 24 radiocarbon samples will be available for calibration of $\overline{R_F}$, $\overline{\delta_F}$ $\overline{\delta_{ff}}$, or $\overline{\delta_{F-tr}}$. With that amount of calibration samples available, due to the large noise of the calibrated footprint-weighted parameters $\overline{\delta_F}$ $\overline{\delta_{ff}}$, or $\overline{\delta_{F-tr}}$ it may be advantageous to group all calibrations to obtain robust annual median values for $\overline{\delta_F}$ $\overline{\delta_{ff}}$, or $\overline{\delta_{F-tr}}$. If a large number of precise radiocarbon measurements are available or if the parameters do not change over the course of several years and thus, several years of calibration samples can be accumulated, it is advantageous to apply radiocarbon calibrations at half-yearly resolution. Note, that due to changes in technology and technical processes, as well as due to a year-to-year variation of extreme temperatures, the contribution from CO_{2F} different sectors are likely to change within a period of four years. However, this could be checked e.g. using night-time Keeling plot intercepts (Vardag et al., in preparation). For calibration of $\overline{R_F}$, integrated $\Delta^{14}C(CO_2)$ calibration could be used with rather small but systematic biases or grab samples could be used for slightly larger, but random uncertainty. The accuracy then will typically be better than 10% for the CO-method or the $\delta^{13}C(CO_2)$ method.

The precision of CO- and $\delta^{13}C(CO_2)$-based approaches is very similar for all site classes, but for polluted sites $\delta^{13}C(CO_2)$ seems slightly more precise. For Heidelberg it is about 25% (e.g. $1\sigma/\mathrm{mean}(y_F)$). For CO, the uncertainty originates mainly from the large variation of $\overline{R_F}$ in our model runs due to the inhomogeneity of fuel CO sources in the footprint area of urban or polluted measurement stations and due to natural CO sources. The uncertainty of the $\delta^{13}C(CO_2)$ approach is mainly determined by the limited measurement precision of $\delta^{13}C(CO_2)$. Thus in order to use $\delta^{13}C(CO_2)$ as a tracer for fuel CO_2 it is vital to perform isotopic measurements with a precision of at least 0.05 ‰. The combination of $\delta^{13}C(CO_2)$ and CO for fuel CO_2 estimation is favorable in cases where each of two emission groups is well distinguishable by one of the tracers. Since for our model setting this is only partly the case (EDGAR emission inventory, see Table A1), the combination of these tracers provides only little additional information.

We have found, that hypothetical future $\Delta^{14}C(CO_2)$ measurements with 5 ‰ precision (see Figure 5f-7f) would generally be a very precise tracer for continuous fuel CO_2 estimation at rural ($1\sigma/\mathrm{mean}(y_F) \approx 90\%$), urban (ca. 20%) and polluted (ca. 10%) stations. The precision of fuel CO_2 estimates is determined mainly by the limited measurement precision of background and total $\Delta^{14}C(CO_2)$ (± 5‰). Note however, that $\Delta^{14}C(CO_2)$ measurements with 5 ‰ precision are not yet fully developed and commercially available. For comparison, a $\Delta^{14}C(CO_2)$ measurement precision of 1% would be needed to achieve a CO_{2F} precision similar to that of $\delta^{13}C(CO_2)$- and CO-based methods. An uncertainty of 2%, which could be a realistic near future precision of laser-based instruments (Galli et al., 2013), would lead to relative uncertainties of 260%, 50% and 30% respectively. The downside of $\Delta^{14}C(CO_2)$ is its inability to determine biofuel CO_2. Therefore, the $\Delta^{14}C(CO_2)$ methods will underestimate the fuel CO_2 (biofuel plus fossil fuel) contributions approximately by the share of biofuel in CO_2 at the site. This may be only a small contribution as was the case for the studied year 2012 (e.g. 5% in Heidelberg), but may increase in the future. Note also that we have not investigated the effect of nuclear power plant $^{14}C(CO_2)$ contributions at the measurement site, which could additionally bias fuel CO_2 estimates derived from $\Delta^{14}C(CO_2)$ measurements. Dispersion model results for Heidelberg (pers. comm. Kuderer, 2015) suggest that the nuclear power facilities (most importantly Philippsburg, located about 25 km south-west of

Heidelberg), increase monthly mean $\Delta^{14}C(CO_2)$ by about (2 ± 2) ‰, corresponding to a misassignment in fuel CO_2 of about 0.8 ± 0.8 µmol/mol (≈ 5%). If there are nuclear power plants or fuel reprocessing plants in the catchment area of the measurement site and if monthly mean emission data of pure $^{14}C(CO_2)$ from these nuclear facilities are available, it is advisable to correct for them at the highest possible temporal resolution e.g. using transport models (Vogel et al., 2013b). Note, that for the calibration of $\overline{R_{\mathrm{F}}}$, $\overline{\delta_{\mathrm{F}}}$ $\overline{\delta_{\mathrm{ff}}}$ or $\overline{\delta_{\mathrm{F-tr}}}$ using $\Delta^{14}C(CO_2)$ grab samples, it should be possible to choose the calibration grab samples via trajectory forecast such that no nuclear power plant influences are encountered in the grab samples. However, this limits the footprint area that can be sampled and calibrated.

We have compared the diurnal cycle of the tracer-based fuel CO_2 estimates for Heidelberg and found that the tracer configurations using CO, $\delta^{13}C(CO_2)$ and $\Delta^{14}C(CO_2)$ were able to reproduce the diurnal cycle well and show a mean difference of better than 5 ± 15 % and a root mean square difference of 15% at the most. This seems surprising, since one might expect a diurnal pattern of $\overline{\delta_{\mathrm{F}}}$ and $\overline{R_{\mathrm{F}}}$ due to a varying share of emissions of different emission sectors in the footprint, leading to a systematic deviation of the estimated from the real modelled diurnal cycle. However, since the diurnal patterns are small (e.g. peak to peak difference of $\delta^{13}C(CO_2)$ ca. 2 ‰), the mean diurnal variations are not significantly improved when using a diurnal correction of the mean isotopic source signatures. One should keep in mind that natural CO contributions may also vary systematically on a diurnal basis. Such a natural systematic variation was not included into the model simulation, but will potentially introduce a diurnal bias into the continuous fuel CO_2 estimate in a real setting. Therefore, it may be necessary to model or approximate natural CO in a real setting. It may be possible to approximate the (sub-monthly) natural CO component using formaldehyde (HCHO) measurements, since the production of CO from NMHC pass HCHO as intermediate molecule (Atkinson, 2000). However, the high dry deposition rate of HCHO may complicate the interpretation further. Since afternoon values are often used in inverse model studies to derive fluxes it is important, that afternoon fuel CO_2 values can be estimated accurately. This could be confirmed for $\delta^{13}C(CO_2)$ and CO in this study (see Fig 8).

In order to better study the biospheric carbon fluxes on all relevant scales, it is important to improve fuel CO_2 bottom-up inventories, so that fuel and biospheric CO_2 can be separated for independent use in inverse model approaches. At present, emission inventories typically have uncertainties of 30-150 % at regional resolution (Wang et al., 2013). We could show in our study that some tracer-based approaches such as CO and $\delta^{13}C(CO_2)$-based methods lead to uncertainties of fuel CO_2 of 30% and accuracies of 10% (after calibration). However, for retrieving improved emission estimates using inverse models, also the model transport errors need to be taken into account and convoluted with the accuracy of fuel CO_2 estimates. At the moment, the model transport errors are usually larger during night time (ca. 100%) than in the afternoon (ca. 40%) (besides at mountain sites), which is why mainly afternoon values are used in model inversions (Gerbig et al., 2008). Obviously, but unfortunately during the afternoon hours, the CO_{2F} signal is very small complicating the unbiased estimation of CO_{2F} emissions using continuous tracers in inverse transport models in these hours until better transport models and boundary layer height models exist.

Acknowledgment: We thank Ute Karstens and Thomas Koch for valuable modelling lessons and help with setting up the model. We are also greatful for valuable discussions on fossil fuel CO_2 in Heidelberg with Felix R. Vogel and Samuel Hammer. We would also like to thank Jocelyn Turnbull and one anonymous referee for their valuable feedback. This work has been funded by the InGOS EU project (284274) and ICOS BMBF project (01LK1225A).

References

Ahmadov, R., Gerbig, C., Kretschmer, R., Koerner, S., Neininger, B., Dolman, A. J. and Sarrat, C.: Mesoscale covariance of transport and CO_2 fluxes: Evidence from observations and simulations using the WRF-VPRM coupled atmosphere-biosphere model, J. Geophys. Res., 112, D22107, doi:10.1029/2007JD008552, 2007.

Atkinson, R.: Atmospheric chemistry of VOCs and NOx, Atmos. Environ., 34, 2063–2101, 2000.

Ballantyne, A. P., Miller, J. B., Baker, I. T., Tans, P. P., and White, J. W. C.: Novel applications of carbon isotopes in atmospheric CO_2: what can atmospheric measurements teach us about processes in the biosphere?, Biogeosciences, 8, 3093-3106, doi:10.5194/bg-8-3093-2011, 2011.

Bousquet, P., Peylin, P., Ciais, P., Le Quéré, C., Friedlingstein, P., & Tans, P. P. : Regional changes in carbon dioxide fluxes of land and oceans since 1980. Science, 290(5495), 1342-1346, 2000.

BP: The role of biofuels beyond 2020, Technical report issued Sept. 2013. Available at: http://www.bp.com/en/global/alternative-energy/our-businesses/biofuels.html, (last access: 23.02.2015)

Conrad R.: Soil microorganisms as controllers of atmospheric trace gases (H_2, CO, CH_4, OCS, N_2O, and NO). Microbiol Rev 60:609–640, 1996.

Coyle, W.: The future of biofuels. Economic Research Service, Washington, DC, 2007.

Denier van der Gon, H.D., Hendriks, C., Kuenen, J., Segers, A., Visschedijk, A.; Description of current temporal emission patterns and sensitivity of predicted AQ for temporal emission patterns, TNP Report, EU FP7 MACC deliverable report D_D-EMIS_1.3. Available at: https://gmes-atmosphere.eu/documents/deliverables/d-emis/MACC_TNO_del_1_3_v2.pdf , 2011.

Djuricin, S., Pataki, D. E. and Xu, X.: A comparison of tracer methods for quantifying CO_2 sources in an urban region, J. Geophys. Res., 115, D11303, doi:10.1029/2009JD012236, 2010.

Dörr, H., B. Kromer, I. Levin, K. O. Münnic, and H.-J. Volpp: CO_2 and radon 222 as tracers for atmospheric transport, J. Geophys. Res., 88(C2), 1309–1313, doi:10.1029/JC088iC02p01309, 1983.

Druffel, E. M., & Suess, H. E.: On the radiocarbon record in banded corals: exchange parameters and net transport of $^{14}CO_2$ between atmosphere and surface ocean. Journal of Geophysical Research: Oceans, 88(C2), 1271-1280, 1983.

European Commission –Joint Research Centre /PBL Netherlands Environmental Assessment Agency. The Emissions Database for Global Atmospheric Research (EDGAR) version 4.3. http://edgar.jrc.ec.europa.eu/, 2015

Esler, M. B., Griffith, D. W. T., Wilson, S. R., and Steele, L. P.: "Precision trace gas analysis by FT-IR spectroscopy. 2. The $^{13}C/^{12}C$ isotope ratio of CO_2." Analytical chemistry 72.1 (2000): 216-221.

Flanagan, L. B., Ehleringer, J. R., and Pataki D. E. (Eds.): Stable isotopes and biosphere-atmosphere interactions, Elsevier Academic Press, San Diego, US, 318 pp., 2005.

Galli, I., Bartalini, S., Cancio, P., De Natale, P., Mazzotti, D., Giusfredi, G., Fedi, M.E. and Mando, P. A.: Optical detection of radiocarbon dioxide: first results and AMS intercomparison. Radiocarbon, 55(2-3), 213-223, 2013.

Gamnitzer, U., Karstens, U., Kromer, B., Neubert, R. E., Meijer, H. A., Schroeder, H., and Levin, I.: Carbon monoxide: A quantitative tracer for fossil fuel CO_2?. J. Geophys. Res. [Atmos.] 111, 2006.

Gerbig, C., Lin, J. C., Wofsy, S. C., Daube, B. C., Andrews, A. E., Stephens, B. B., Bakwin, P. S. and Grainger, C. A.: Toward constraining regional-scale fluxes of CO2 with atmospheric observations over a continent: 2. Analysis of COBRA data using a receptor-oriented framework, J Geophys Res-Atmos, 108(D24), doi:10.1029/2003JD003770, 2003.

Gerbig, C., Körner, S. and Lin, J. C.: Vertical mixing in atmospheric tracer transport models: error characterization and propagation, Atmos. Chem. Phys., 8, 591–602, 2008.

Granier, C., Pétron, G., Müller, J.-F. and Brasseur, G. : The impact of natural and anthropogenic hydrocarbons on the tropospheric budget of carbon monoxide. Atmos. Environ. 34, 5255–5270, 2000.

Graven, H. D., and Gruber. N.: Continental-scale enrichment of atmospheric $^{14}CO_2$ from the nuclear power industry: potential impact on the estimation of fossil fuel-derived CO_2. Atmos. Chem. Phys. 11, 12339-12349, 2011.

Gros, V., Tsigaridis, K., Bonsang, B:, Kanakidou, M., Pio, C.: Factors controlling the diurnal variation of CO above a forested area in southeast Europe, Atmos. Environ. 36, 19, 3127-3135, ISSN 1352-2310, 2002.

Gurney, K. R., Law, R. M., Denning, A. S., Rayner, P. J., Baker, D., Bousquet, P., Bruhwiler, L., Chen, Y., Ciais, C., Fan, S., Fung, I. Y., Gloor, M., Heimann, M., Higuchi, John,J., Maki,T., Maksyutov, S., Masarie,K., Peylin, P., Prather, M., P, B.C., Randerson, J., Sarmiento, J., Taguc, S., Takahashi, T., & Yuen, C. W. :Towards robust regional estimates of CO_2 sources and sinks using atmospheric transport models. Nature, 415(6872), 626-630, 2002.

Gurney, K. R., Y.-H. Chen, T. Maki, S. R. Kawa, A. Andrews, and Z. Zhu: Sensitivity of atmospheric CO_2 inversions to seasonal and interannual variations in fossil fuel emissions, J. Geophys. Res., 110, D10308, doi:10.1029/2004JD005373, 2005.

Hammer, S., Griffith, D. W. T., Konrad, G., Vardag, S., Caldow, C., and Levin, I.: Assessment of a multi-species in situ FTIR for precise atmospheric greenhouse gas observations, Atmos. Meas. Tech., 6, 1153-1170, doi:10.5194/amt-6-1153-2013, 2013.

Heimann, M., and Koerner, S.: The global atmospheric tracer model TM3, Technical Reports, Max-Planck-Institute for Biogeochemie, 5, 131 pp., 2003.

IEA, International Energy Agency: Key World Energy Statistics 2014, 2014, available at: http://www.iea.org/publications/freepublications/publication/key-world-energy-statistics-2014.html (last access: 30 Sept. 2015).

Inman, R. E., Ingersoll, R. B., Levy, E. A. : Soil: A natural sink for carbon monoxide, Science, 172(3989), 1229–1231, doi:10.1126/science.172.3989.1229, 1971.

Jung, M., Henkel, K., Herold, M., and Churkina, G.: Exploiting synergies of global land cover products for carbon cycle modeling, Remote Sens. Environ., 101, 534–553, 2006.

Kaul, M.: Isotopenverhältnisse im atmosphärischem Kohlendioxid und seine Quellen im Raum Heidelberg, Staatsexamensarbeit, 2007.

Keeling, C. D., The concentration and isotopic abundances of atmospheric carbon dioxide in rural areas, Geochim Cosmochim Acta, 13, 322– 334, 1958.

Keeling, C. D., The concentration and isotopic abundance of carbon dioxide in rural and marine air, Geochim. Cosmochim. Acta, 24, 277– 298, 1961.

Keeling, R. F., Piper, S.C. and Heimann, M.: Global and hemispheric CO_2 sinks deduced from changes in atmospheric O_2 concentration, Nature 381, 218-221, 1996.

Le Quéré, C., Moriarty, R., Andrew, R. M., Peters, G. P., Ciais, P., Friedlingstein, P., Jones, S. D., Sitch, S., Tans, P., Arneth, A., Boden, T. A., Bopp, L., Bozec, Y., Canadell, J. G., Chini, L. P., Chevallier, F., Cosca, C. E., Harris, I., Hoppema, M., Houghton, R. A., House, J. I., Jain, A. K., Johannessen, T., Kato, E., Keeling, R. F., Kitidis, V., Klein Goldewijk, K., Koven, C., Landa, C. S., Landschützer, P., Lenton, A., Lima, I. D., Marland, G., Mathis, J. T., Metzl, N., Nojiri, Y., Olsen, A., Ono, T., Peng, S., Peters, W., Pfeil, B., Poulter, B., Raupach, M. R., Regnier, P., Rödenbeck, C., Saito, S., Salisbury, J. E., Schuster, U., Schwinger, J., Séférian, R., Segschneider, J., Steinhoff, T., Stocker, B. D., Sutton, A. J., Takahashi, T., Tilbrook, B., van der Werf, G. R., Viovy, N., Wang, Y.-P., Wanninkhof, R., Wiltshire, A., and Zeng, N.: Global carbon budget 2014, Earth Syst. Sci. Data, 7, 47-85, doi:10.5194/essd-7-47-2015, 2015.

Levin, I., Kromer, B., Schmidt, M., and Sartorius, H.: A novel approach for independent budgeting of fossil fuel CO_2 over Europe by $^{14}CO_2$ observations, Geophys. Res. Lett., 30(23), 2194, doi:10.1029/2003GL018477, 2003.

Levin, I. and Karstens, U.: Inferring high-resolution fossil fuel CO_2 records at continental sites from combined (CO_2)-C-14 and CO observations, Tellus B, 59, 245–250, doi:10.1111/j.1600-0889.2006.00244.x, 2007.

Levin, I., Hammer, S., Kromer, B., Meinhardt, F.: Radiocarbon observations in atmospheric CO_2: Determining fossil fuel CO_2 over Europe using Jungfraujoch observations as background, Sci. Total Environ. 391, 211-216, ISSN 0048-9697, 2008.

Levin, I., Naegler, T., Kromer, B., Diehl, M., Francey, R. J., Gomez-Pelaez, A. J., Steele, L.P., Wagenbach, D., Weller, R. and Worthy, D. E.: Observations and modelling of the global distribution and long-term trend of atmospheric $^{14}CO_2$. *Tellus B*, *62*(1), 26-46, 2010.

Levin, I., Kromer, B., Hammer, S.: Atmoposheric $\Delta^{14}CO_2$ trend in Western European background air from 2000 to 2012, Tellus B, 2013.

Lin, J. C., C. Gerbig, S. C. Wofsy, A. E. Andrews, B. C. Daube, K. J. Davis, and C. A. Grainger (2003), A near-field tool for simulating the upstream influence of atmospheric observations: The

Stochastic Time-Inverted Lagrangian Transport (STILT) model, J. Geophys. Res., 108, 4493, doi:10.1029/2002JD003161, D16.

Mahadevan, P., Wofsy, S. C., Matross, D. M., Xiao, X., Dunn, A. L., Lin, J. C., Gerbig, C., Munger, J. W., Chow, V. Y., and Gottlieb, E. W.: A satellite-based biosphere parameterization for net ecosystem CO_2 exchange: Vegetation Photosynthesis and Respiration Model (VPRM), Global Biogeochem. Cycles, 22, doi:10.1029/2006GB002735, 2008.

Marland, G., Brenkert, A. and Olivier, J. (1999) CO2 from fossil fuel burning: a comparison of ORNL and EDGAR estimates of national emissions. Environmental Science & Policy 2, 265-273, doi:10.1016/s1462-9011(99)00018-0.

McIntyre, C. P., McNicholm, A. P., Roberts, M.L., Seewald, J.S., von Reden, K.F., and Jenkins, W.J..: Improved Precision of ^{14}C Measurements for CH_4 and CO_2 Using GC and Continuous-Flow AMS Achieved by Summation of Repeated Injections. Radiocarbon, 55, 2013.

Meijer, H. A. J., Smid, H. M. , Perez, E. Keizer, M. G.: Isotopic characterization of anthropogenic CO_2 emissions using isotopic and radiocarbon analysis, Phys. Chem. Earth, 21(5–6), 483–487, 1996.

Miller, J. B., Lehman, S. J., Montzka, S. A., Sweeney, C., Miller, B. R., Karion, A., Wolak, C., Dlugokencky, E.J., Southon, J., Turnbull, J. C and Tans, P. P.: Linking emissions of fossil fuel CO_2 and other anthropogenic trace gases using atmospheric $^{14}CO_2$, J. Geophys. Res., 117, D08302, doi:10.1029/2011JD017048, 2012.

Mook, W. M. E. 2001. Environmental Isotopes in the Hydrological Cycle. Principles and Applications. UNESCO/IAEA Series, http://www.naweb.iaea.org/napc/ih/IHS_resources_publication_hydroCycle_en.html

Newman, S., Jeong, S., Fischer, M. L., Xu, X., Haman, C. L., Lefer, B., Alvarez, S., Rappenglueck, B., Kort, E. A., Andrews, A. E., Peischl, J., Gurney, K. R., Miller, C. E., and Yung, Y. L.: Diurnal tracking of anthropogenic CO_2 emissions in the Los Angeles basin megacity during spring 2010, Atmos. Chem. Phys., 13, 4359-4372, doi:10.5194/acp-13-4359-2013, 2013.

Nydal, R., Lövseth, K. and Gullicksen, S.: A survey of radiocarbon variation in nature since the test ban treaty. University of California Press, Berkley, California, 1979.

Parrish, D. D., Trainer, M., Holloway, J.S., Yee, J., Warshawsky, S., Fehsenfeld, F., Forbes,G., Moody, J.: Relationships between ozone and carbon monoxide at surface sites in the North Atlantic region, J. Geophys. Res., 103(D11), 13,357–13,376, doi:10.1029/98JD00376, 1993.

Pataki, D. E., Ehleringer, J. R., Flanagan, L. B., Yakir, D., Bowling, D. R., Still, C. J., Buchmann, N. , Kaplan, J. O. and Berry, J. A.: The application and interpretation of Keeling plots in terrestrial carbon cycle research, Global Biogeochem. Cycles, 17, 1022, doi:10.1029/2001GB001850, 1, 2003.

Pataki, D. E., Alig, R. J., Fung, A. S., Golubiewski, N. E., Kennedy, C. A., McPherson, E. G., Nowak, D. J., Pouyat, R. V., and Romero Lankao, P.: Urban ecosystems and the North American carbon cycle, Global Change Biol., 12, 2092–2102, doi:10.1111/j.1365-2486.2006.01242.x, 2006.

Peylin, P., Houweling, S., Krol, M. C., Karstens, U., Rödenbeck, C., Geels, C., Vermeulen, A., Badawy, B., Aulagnier, C., Pregger, T., Delage, F., Pieterse, G., Ciais, P., and Heimann, M.: Importance of fossil fuel emission uncertainties over Europe for CO_2 modeling: model intercomparison, Atmos. Chem. Phys., 11, 6607-6622, doi:10.5194/acp-11-6607-2011, 2011.

Peylin, P., Law, R. M., Gurney, K. R., Chevallier, F., Jacobson, A. R., Maki, T., Niwa, Y., Patra,

P. K., Peters, W., Rayner, 5 P. J., Rödenbeck, C., van der Laan-Luijkx, I. T., and Zhang, X.: Global atmospheric carbon budget: results from an ensemble of atmospheric CO_2 inversions, Biogeosciences, 10, 6699–6720, doi:10.5194/bg-10-6699-2013, 2013. 8885, 8887, 2013.

Prather, M., Ehhalt, D., Dentener, F., Derwent, R. G., Dlugokencky, E., Holland, E., Isaksen, I. S. A., Katima, J., Kirchhoff, V., Matson, P., Midgley, P. M., and Wang, M.: Atmospheric chemistry and greenhouse gases, in: Climate Change 2001, edited by: Houghton, J. T., 239–287, Cambridge Univ. Press, New York, 2001.

Rödenbeck, C.: Estimating CO2 sources and sinksfrom atmospheric mixing ratio measurements using a global inversion of atmospheric transport, Max Planck Institute for Biogeochemistry, Jena, Germany. [online] Available from: http://www.bgc-jena.mpg.de/bgc-systems/pmwiki2/uploads/Publications/6.pdf, 2005.

Rogelj, J., McCollum, D., Smith, S., Calvin, K., Clarke, L., Garg, A., Jiang, K., Krey, V., Lowe, J., Riahi, K., Schaeffer, M., van Vuuren, D., Wenying, C., Crippa, M., Janssens-Maenhout, G., Chapter 2 of The emission gap report 2014: What emission levels will comply with temperature limit. In: The emission gap report 2014: a UNEP synthesis report. United Nations Environment Programme (UNEP); 2014

Rivier, L., Ciais, P., Hauglustaine, D. A., Bakwin, P., Bousquet, P, Peylin, P., & Klonecki, A.: Evaluation of SF_6, C_2Cl_4 and CO to approximate fossil fuel CO_2 in the Northern Hemisphere using a chemistry transport model. J. Geophys. Res. 111, D16311, doi:10.1029/2005JD006725, 2006.

Schmidt, A., Rella, C. W., Göckede, M., Hanson, C., Yang, Z., Law, B.E.: Removing traffic emissions from CO_2 time series measured at a tall tower using mobile measurements and transport modeling, Atmospheric Environment, Volume 97, Pages 94-108, ISSN 1352-2310, http://dx.doi.org/10.1016/j.atmosenv.2014.08.006, 2014.

Steinbach, J., Gerbig, C., Rödenbeck, C., Karstens, U., Minejima, C. and Mukai, H.: The CO2 release and Oxygen uptake from Fossil Fuel Emission Estimate (COFFEE) dataset: effects from varying oxidative ratios, Atmos. Chem. Phys., 11(14), 6855–6870, doi:10.5194/acp-11-6855-2011, 2011.

Stohl, A., Forster, C., Frank, A., Seibert, P., Wotawa, G.: Technical note: the Lagrangian particle dispersion model FLEXPART version 6.2. Atmos Chem Phys 5:2461–2474, 2005.

Stuiver, M., and Polach H.A.: Reporting of C-14 data-Discussion. Radiocarbon 19, 355-363, 1977.

Stuiver, M., and Quay, P. D.: Atmospheric ^{14}C changes resulting from fossil fuel CO_2 release and cosmic ray flux variability. Earth and Planet. Sci. Lett. 53, 349-362, 1981.

Suess, H. E: Radiocarbon concentration in modern wood. Science 122, 415-417, 1955.
Taylor, A. J., Lai, C. T., Hopkins, F. M., Wharton, S., Bible, K., Xu, X., Philipps, C., Bush.S. and Ehleringer, J. R.: Radiocarbon-Based Partitioning of Soil Respiration in an Old-Growth Coniferous Forest. Ecosystem*s*, 1-12, 2015.

Trusilova, K., Roedenbeck, C., Gerbig, C. and Heimann, M.: Technical Note: A new coupled system for global-to-regional downscaling of CO2 concentration estimation, Atmos. Chem. Phys., 10(7), 3205–3213, 2010.

Turnbull, J. C., Miller, J. B., Lehman, S. J., Tans, P. P., Sparks, R. J. and Southon, J.: Comparison of $^{14}CO_2$, CO, and SF_6 as tracers for recently added fossil fuel CO_2 in the atmosphere and implications for biological CO_2 exchange. Geophys. Res. Lett., **33**, L01817, doi: 10.1029/2005GL024213, 2006.

Turnbull, J. C., S. J. Lehman, J. B. Miller, R. J. Sparks, J. R. Southon, and P. P. Tans : A new high precision $^{14}CO_2$ time series for North American continental air, J. Geophys. Res., 112, D11310, doi:10.1029/2006JD008184, 2007.

Turnbull, J.C., Karion, A., Fischer, M.L., Faloona, I., Guilderson, T., Lehman, S.J., Miller, B.R., Miller, J.B., Montzka, S., Sherwood, T., Saripalli, S., Sweeney, C., Tans, P.P.,: Assessment of fossil fuel carbon dioxide and other anthropogenic trace gas emissions from airborne measurements over Sacramento, California in spring 2009. Atmos. Chem. Phys. 11, 705-721, 2011.

Turnbull, J. C., Sweeney, C., Karion, A., Newberger, T., Lehman, S. J., Tans, P. P., Davis, K. J., Lauvaux, T., Miles, N. L., Richardson, S. J., Cambaliza, M. O., Shepson, P. B., Gurney, K., Patarasuk, R. Razlivanov, I.: Toward quantification and source sector identification of fossil fuel CO_2 emissions from an urban area: Results from the INFLUX experiment. Journal of Geophysical Research: Atmospheres, 2015.

Tuzson, B., Henne, S., Brunner, D., Steinbacher, M., Mohn, J., Buchmann, B., & Emmenegger, L.: Continuous isotopic composition measurements of tropospheric CO_2 at Jungfraujoch (3580 m asl), Switzerland: real-time observation of regional pollution events. Atmos. Chem. Phys., 11(4), 1685-1696, 2011.

Vardag, S. N., Hammer, S., O'Doherty, S., Spain, T. G., Wastine, B., Jordan, A., and Levin, I.: Comparisons of continuous atmospheric CH_4, CO_2 and N_2O measurements – results from a travelling instrument campaign at Mace Head, Atmos. Chem. Phys., 14, 8403-8418, doi:10.5194/acp-14-8403-2014, 2014.

Vogel, F. R.:$^{14}CO_2$-calibrated carbon monoxide as proxy to estimate the regional fossil fuel CO_2 component at hourly resolution. PhD thesis, Ruprecht-Karls University Heidelberg, Germany, 2010.

Vogel, F., Hammer, S., Steinhof, A., Kromer, B., & Levin, I.: Implication of weekly and diurnal ^{14}C calibration on hourly estimates of CO-based fossil fuel CO_2 at a moderately polluted site in southwestern Germany. *Tellus B, 62*(5). doi: http://dx.doi.org/10.3402/tellusb.v62i5.16600, 2010.

Vogel, F. R., Huang, L., Ernst, D., Giroux, L., Racki, S., & Worthy, D. E. J.: Evaluation of a cavity ring-down spectrometer for in situ observations of $^{13}CO_2$. Atmospheric Measurement Techniques, 6(2), 301-308, 2013a.

Vogel, F., Levin, I., WorthyY, D.: Implications for Deriving Regional Fossil Fuel CO_2 Estimates from Atmospheric Observations in a Hot Spot of Nuclear Power Plant $^{14}CO_2$ Emissions. Radiocarbon**,** North America, 55, may. 2013b.

Wang, R., Tao, S., Ciais, P., Shen, H.Z., Huang, Y., Chen,H., Shen, G.F. , Wang, B., Li, W., Zhang, Y. Y., Lu, Y., Zhu, D., Chen, Y.C., Liu, X.P., Wang, W.T., Wang, X.L., Liu, W.X. Li, B.G. , Piao, S.L.: High-resolution mapping of combustion processes and implications for CO_2 emissions, Atmos. Chem. Phys., 13, pp. 1–15, 2013.

Widory, D., Proust, E., Bellenfant, G., Bour, O.: Assessing methane oxidation under landfill covers and its contribution to the above atmospheric CO_2 levels: The added value of the isotope ($\delta^{13}C$ and $\delta^{18}O$ CO2; $\delta^{13}C$ and δD CH_4) approach, Waste Manage, 32, 9, 1685-1692, 0956-053X, 2012, Available at: http://www.sciencedirect.com/science/article/pii/S0956053X12001729.

Zondervan, A. and Meijer, H. A. J.: Isotopic characterisation of CO_2 sources during regional pollution events using isotopic and radiocarbon analysis. Tellus B, 48: 601–612. doi: 10.1034/j.1600-0889.1996.00013.x,1996.

Appendix

A) Methods of continuous fuel CO_2 determination

A.1. Tracer configurations and their emission groups

We formally introduce six different tracers or tracer combinations, which we use to estimate fuel CO_2 continuously: CO_2 is used as sole tracer for fuel CO_2. CO, $\delta^{13}C(CO_2)$ and $\Delta^{14}C(CO_2)$ records are each used solely with CO_2 to estimate fuel CO_2. Further, CO is used as tracer for traffic (and $\delta^{13}C(CO_2)$ as tracer for fuel CO_2 minus traffic) and finally CO is used as tracer for biofuels (and $\delta^{13}C(CO_2)$ as tracer for fuel CO_2 minus biofuels). The different emission groups are also listed and characterized in Table A1.

A.1.1. CO_2 as sole tracer for fuel CO_2

When using CO_2 alone as "tracer" for fuel CO_2 ($y_F = y_{ff} + y_{bf}$), the total regional CO_2 offset is assumed to solely originate from fuel emissions:

$$y_F = \Delta y \tag{A1}$$

With $\Delta y = y_{tot} - y_{bg.}$

This simple approach is valid, if (nearly) all CO_2 emissions are from fuel burning, as might be the case in cold winters or in areas without biospheric activity (e.g. Mega cities).

A.1.2. CO as tracer for fuel CO_2

The CO offset ($\Delta x = x_{tot} - x_{bg}$) can be used to estimate fuel CO_2 offset if it is divided by the mean ratio $\overline{R_F} = \Delta x / \Delta y_F$ of all fuel sources:

$$y_F = \frac{\Delta x}{\overline{R_F}} \tag{A2}$$

Note that in reality the ratio $\overline{R_F}$ varies, depending on the share of emissions of different emission sectors in the catchment area, their temporal emission patterns, and due to natural CO sources and sinks, at least in summer (Prather et al., 2001). We denote $\overline{R_F}$ with an overbar to emphasize that this is a footprint-weighted average of the fuel emission ratio.

A.1.3. CO as tracer for traffic CO_2 and $\delta^{13}C(CO_2)$ *as tracer for all fuel CO_2, except for traffic CO_2*

We now include $\delta^{13}C(CO_2)$ in fuel CO_2 estimation as a tracer for all fuel CO_2 except those of traffic ($y_{\text{F-tr}} = y_{\text{ff}} + y_{\text{bf}} - y_{\text{tr}}$).

$$y_{\text{tot}} = y_{\text{bg}} + y_{\text{bio}} + y_{\text{tr}} + y_{\text{F-tr}} \tag{A3}$$

$$y_{\text{tot}}\delta_{\text{tot}} = y_{\text{bg}}\delta_{\text{bg}} + y_{\text{bio}}\delta_{\text{bio}} + y_{\text{tr}}\overline{\delta_{\text{tr}}} + y_{\text{F-tr}}\overline{\delta_{\text{F-tr}}} \tag{A4}$$

In analogy to $\overline{R_F}$ we denote $\overline{\delta_{\text{tr}}}$ and $\overline{\delta_{\text{F-tr}}}$ with an overbar to emphasize that these are footprint-weighted averages of the emission groups traffic CO_2 and fuel CO_2 excluding traffic, respectively. Solving Eq. (A3) for y_{bio}, we can substitute y_{bio} in Eq. (A4). In analogy to Eq. (A2), we use CO as tracer for traffic CO_2:

$$y_{tr}(t) = \frac{x_{\text{tr}}(\text{t})}{\overline{R_{\text{tr}}}} \tag{A5}$$

With the mean $\Delta CO/\Delta CO_2$ ratio of traffic $\overline{R_{\text{tr}}} = (\Delta x/\Delta y)_{\text{tr}}$. CO_{tr} can be determined from:

$$\text{CO}_{\text{tr}}(\text{t}) = \Delta\text{CO}(\text{t}) \cdot \overline{m_{\text{tr}}} \tag{A6}$$

with $\overline{m_{tr}} = (\Delta x_{\text{tr}}/\Delta x)$ being the share of traffic CO to the total CO offset. $\overline{m_{tr}}$ needs to be estimated from bottom-up inventories and can be found in Table A1 (right column) and is also dependent on the footprint area of the measurement site and the sources and sinks lying in this area. Eq. (A3) – Eq. (A6) can then be re-arranged:

$$y_{\text{F-tr}} = \frac{y_{\text{tot}}\delta_{\text{tot}} - y_{\text{bg}}\delta_{\text{bg}} - (y_{\text{tot}} - y_{\text{bg}} - y_{\text{tr}})\delta_{\text{bio}} - y_{2\text{tr}}\overline{\delta_{\text{tr}}}}{\overline{\delta_{\text{F-tr}}} - \delta_{\text{bio}}} \tag{A7}$$

Total fuel CO_2 (y_F) contribution can then be determined as the sum of y_{tr} (Eq. (A5)) and $y_{\text{F-tr}}$ (Eq. (A7)).

A.1.4. CO as tracer for biofuel CO_2 and δ^{13}C(CO_2) *as tracer for all fuel CO_2, except for biofuel CO_2*

This method of fuel CO_2 estimation is in analogy to case A.1.3, but instead of separating fuel CO_2 in to traffic contributions (y_{tr}) and others ($y_{\mathrm{F\text{-}tr}}$), we separate it into biofuel contributions (y_{bf}) and others ($y_{\mathrm{F\text{-}bf}} = y_{\mathrm{ff}}$); this leads to:

$$\mathrm{y}_{\mathrm{F-bf}} = \frac{y_{\mathrm{tot}}\delta_{\mathrm{tot}} - y_{\mathrm{bg}}\delta_{\mathrm{bg}} - (y_{\mathrm{tot}} - y_{\mathrm{bg}} - y_{\mathrm{bf}})\delta_{\mathrm{bio}} - y_{\mathrm{bf}}\overline{\delta_{\mathrm{bf}}}}{\overline{\delta_{\mathrm{ff}}} - \delta_{\mathrm{bio}}} \tag{A8}$$

Analogously to Eq. (A10), we formulate for y_{bf}:

$$y_{\mathrm{bf}}(\mathrm{t}) = \frac{\Delta x(\mathrm{t}) \cdot \overline{m_{\mathrm{bf}}}}{\overline{R_{\mathrm{bf}}}} \tag{A9}$$

With $\overline{m_{\mathrm{bf}}} = (\Delta x_{\mathrm{bf}}/\Delta x)$ from bottom-up inventories (see Table A1). Total fuel CO_2 (y_{F}) is calculated as the sum of y_{bf} (Eq. (A9)) and $y_{\mathrm{F\text{-}bf}}$ (Eq. (A9)).

A.1.5. δ^{13}C(CO_2) *as sole tracer for fuel emission*

When using δ_{tot} as tracer for all fuel contributions, Eq. (A3) and Eq. (A4) simplify to

$$y_{\mathrm{F}} = \frac{y_{\mathrm{tot}}\delta_{\mathrm{tot}} - y_{\mathrm{bg}}\delta_{\mathrm{bg}} - (y_{\mathrm{tot}} - y_{\mathrm{bg}})\delta_{\mathrm{bio}}}{\overline{\delta_{\mathrm{F}}} - \delta_{\mathrm{bio}}} \tag{A10}$$

if all fuel CO_2 ($y_{\mathrm{F\text{-}tr}}$ and y_{tr}) contributions are pooled to y_{F}.

A.1.6. Δ^{14}C(CO_2) *as tracer for fossil fuel CO_2*

Following Levin et al. (2008), we can derive fossil fuel CO_2 from Δ^{14}C(CO_2)and total CO_2 measurements according to:

$$y_{\mathrm{ff}} = \frac{y_{\mathrm{bg}}\left(\Delta^{14}\mathrm{C}_{\mathrm{bg}} - \Delta^{14}\mathrm{C}_{\mathrm{bio}}\right) - y_{\mathrm{tot}}(\Delta^{14}\mathrm{C}_{\mathrm{tot}} - \Delta^{14}\mathrm{C}_{\mathrm{bio}}) - y_{\mathrm{bf}}(\Delta^{14}\mathrm{C}_{\mathrm{bio}} - \Delta^{14}\mathrm{C}_{\mathrm{bf}})}{1 + \Delta^{14}\mathrm{C}_{\mathrm{bio}}}$$

(A11)

However, since $\Delta^{14}C_{bio} \approx \Delta^{14}C_{bf}$, and because biofuel contributions are not known, we neglect the last term of the numerator in the following. Note, that since $\Delta^{14}C(CO_2)$is not sensitive to biofuel contributions, it is only possible to estimate the fossil fuel CO_2 contributions without biofuel contributions.

A.2 Determination of parameters and variables

The background values y_{bg}, x_{bg}, δ_{bg} and $\Delta^{14}C_{bg}$ should represent the regional clean air to which the source contributions from the footprint area are added. Since often, there are no nearby clean-air observations available for a polluted station, we use those mole fractions as background where the air masses in the boundary layer are well mixed with the free troposphere. This is usually the case in the afternoon and is associated with low mole fractions. Since CO_2, as well as CO both have local sinks relevant on the timescale of days, we here use CH_4 as an indicator for a well-mixed boundary layer and assume that, when the CH_4 mole fraction reaches a minimum value (within two days), vertical mixing is strongest. Principally, if continuous radon measurements were available, these could also be used as an indicator for vertical mixing (Dörr et al., 1983), instead of CH_4. We checked that the CH_4 minimum values always represent a lower envelope of the simulated greenhouse gas record and does not vary at the synoptic time scale. We then use the total mole fractions and isotopic records y_{tot}, $x_{tot,}$ δ_{tot}, and $\Delta^{14}C_{tot}$ observed during situations with minimal CH_4 mole fractions as background values.

Further, in order to solve Eq. (A2)- Eq. (A11), we need the input parameters $\delta_{bio,}$ $\Delta^{14}C_{bio}$. These input parameters were assigned with the objective to create realistic modelled data set (see Table 1 and A1). Additionally, the integrated footprint-weighted parameters $\overline{R_{\mathrm{F}}}$, $\overline{R_{\mathrm{tr}}}$, $\overline{R_{\mathrm{bf}}}$, $\overline{\delta_{\mathrm{F}}}$ $\overline{\delta_{\mathrm{ff}}}$, $\overline{\delta_{\mathrm{bf}}}$, $\overline{\delta_{\mathrm{tr}}}$, $\overline{\delta_{\mathrm{bio}}}$, $\overline{\delta_{\mathrm{F-tr}}}$, $\overline{m_{\mathrm{bf}}}$ and $\overline{m_{\mathrm{tr}}}$ are required (see Table A1). We call these parameters footprint-weighted, since the ratios and isotopic signatures depend on the relative contribution from the different emission sectors (with their sector specific emission ratios and isotopic signatures) within the footprint of the measurement site. We denote the integrated footprint-weighted parameters with an overbar to draw attention to the fact that the parameters are averaged over the (e.g. monthly) footprint area. Even though the emission factors of the source categories used here are fixed for every pixel, integrated footprint-weighted $\overline{R_{\mathrm{F}}}$, $\overline{R_{\mathrm{tr}}}$, $\overline{R_{\mathrm{bf}}}$, $\overline{\delta_{\mathrm{F}}}$

$\overline{\delta_{\mathrm{ff}}}, \overline{\delta_{\mathrm{bf}}}, \overline{\delta_{\mathrm{tr}}}, \overline{\delta_{\mathrm{bio}}}, \overline{\delta_{\mathrm{F-tr}}}, \overline{m_{\mathrm{bf}}}$ and $\overline{m_{\mathrm{tr}}}$ are not constant in time, because the footprint of the measurement site and the emission patterns are temporally variable. Thus, the footprint-weighted parameters change when the emissions from the different sectors or the footprint of the measurement site vary. Note, that for our model study we do not require the parameters to be absolutely correct, since we do not compare them to measured data. However, since we want to provide a realistic case study, we seek to use the most realistic parameters (see values in Table 1 and A1).

B) "Calibration" with Δ^{14}C(CO$_2$)

Solving Eq. (A3), (A8), (A9) and (A11) for fuel CO$_2$ requires $\overline{R_{\mathrm{F}}}$, $\overline{\delta_{\mathrm{F}}}$ $\overline{\delta_{\mathrm{ff}}}$, and $\overline{\delta_{\mathrm{F-tr}}}$. If these values are not known, they may be derived from Δ^{14}C(CO$_2$)observations (what we then call Δ^{14}C(CO$_2$)-calibrated). However, for the calibration y_{ff} must be known. The idea is to calibrate fossil fuel CO$_2$, e.g. with precise Δ^{14}C(CO$_2$)measurements, on a lower time resolution (e.g. monthly) and assume that the footprint-weighted parameters $\overline{R_{\mathrm{F}}}$, $\overline{\delta_{\mathrm{F}}}$ $\overline{\delta_{\mathrm{ff}}}$, and $\overline{\delta_{\mathrm{F-tr}}}$ do not change significantly within this calibration interval.

Re-arranging Eq. (1) and (2) for $\overline{\delta_{\mathrm{ff}}}$ and averaging it monthly leads to

$$\overline{\delta_{ff}} = \frac{y_{\mathrm{tot}}\delta_{\mathrm{tot}} - y_{\mathrm{bg}}\delta_{\mathrm{bg}} - (y_{\mathrm{tot}} - y_{\mathrm{bg}} - y_{\mathrm{ff}} - y_{\mathrm{bf}})\delta_{\mathrm{bio}} - y_{\mathrm{bf}}\overline{\delta_{\mathrm{bf}}}}{y_{\mathrm{ff}}} \tag{B1}$$

, which could then be used in Eq. (A9). Note that we require the biofuel CO$_2$ in addition to the fossil fuel CO$_2$ from Δ^{14}C(CO$_2$)..

$\overline{\delta_{\mathrm{F}}}$ can then be derived, if the y_{bf} concentration is known.

$$\overline{\delta_{\mathrm{F}}} = \frac{\overline{\delta_{\mathrm{ff}}}y_{\mathrm{ff}} + \overline{\delta_{\mathrm{bf}}}\, y_{\mathrm{bf}}}{y_{\mathrm{ff}} + y_{\mathrm{bf}}} \tag{B2}$$

If fossil fuel emissions are divided into fossil fuel contributions without traffic ($y_{\mathrm{F-tr}}$) and traffic contributions (y_{tr}), we can derive $\overline{\delta_{\mathrm{F-tr}}}$ required for solving Eq (A8):

$$\overline{\delta_{\mathrm{F-tr}}} = \frac{\overline{\delta_{\mathrm{F}}} y_{\mathrm{F}} - \overline{\delta_{\mathrm{tr}}}\, y_{\mathrm{tr}}}{y_{\mathrm{F}} - y_{\mathrm{tr}}} \tag{B3}$$

Analogously, the ratio $\overline{R_{\mathrm{F}}}$ could be calibrated following:

$$\overline{R_{\mathrm{F}}} = \frac{\Delta x}{\Delta y_{\mathrm{F}}} \tag{B4}$$

In order to calculate the monthly mean value of $\langle\overline{\delta_{\mathrm{F}}}\rangle$ and $\langle\overline{R_{\mathrm{F}}}\rangle$, the mean ratios $\langle\frac{\Delta x}{\Delta yF}\rangle$ (Eq. (B1)-(B4)) are needed. However, from integrated $\Delta^{14}C(CO_2)$ sampling, we only have the mean fossil fuel CO_2 and fuel CO_2 values and can thus, only calculate $\frac{\langle\Delta x\rangle}{\langle\Delta yF\rangle}$. Using the product (or ratio) of the means rather than the mean of the product (ratio) is only correct if the factors are uncorrelated. Since, the factors in Eq. (B1) - (B4) (and Δx and Δy_{ff}) are correlated, the integrated calibration cannot be applied without introducing a bias into monthly mean $\langle\overline{\delta_{\mathrm{F}}}\rangle$, $\langle\overline{\delta_{\mathrm{ff}}}\rangle$, $\langle\overline{\delta_{\mathrm{F-tr}}}\rangle$ and $\langle\overline{R_{\mathrm{F}}}\rangle$. Instead of using integrated $\Delta^{14}C(CO_2)$ samples in order to obtain the monthly fossil fuel CO_2 values, it is possible to take grab samples, analyse these for $\Delta^{14}C(CO_2)$ (and with that y_{ff}), total CO_2, $\delta^{13}C(CO_2)_{\mathrm{tot}}$ and CO in order to calculate the individual (non-averaged) values for $\overline{\delta_{\mathrm{F}}}$, $\overline{\delta_{\mathrm{F-tr}}}$, $\overline{\delta_{\mathrm{ff}}}$ and $\overline{R_{\mathrm{F}}}$ (see Sect. 4).

C) Influence of more depleted fuel $\delta^{13}C(CO_2)$ signatures

We have argued that we only require a realistic set of input parameters, rather than an absolutely correct set of parameters to estimate uncertainties of the different tracer methods. However, the results presented so far are to some degree dependent on the emission characteristics used in our model (see Table A1). When using CO as tracer for fuel CO_2, it would be advantageous if natural sources of CO were negligible and if the emission ratio $\overline{R_{\mathrm{F}}}$ would be the same for all sources. When using CO_2 as tracer for fuel CO_2, biospheric CO_2 emissions should be negligible, and when using $\delta^{13}C(CO_2)$, it would be advantageous if fuel CO_2 emissions were strongly depleted compared to biospheric emissions. It is beyond the scope of this work, to show explicitly for all cases how the "choice" of different emission characteristics influences the fuel CO_2 estimate in terms of precision and accuracy. However, in Figure A1, we illustrate exemplary for this latter case how the presence of more depleted fuel sources in the footprint area of the measurement site could improve the tracer $\delta^{13}C(CO_2)$ for fuel CO_2 estimation. This should serve as an example, showing how much the emission characteristics at a site may influence the precision of fuel CO_2 estimates using different tracer configurations.

Figure A1 shows that fuel CO_2 can be estimated much better when the mean source mix in the catchment area of the measurement site exhibits a strongly depleted isotopic source signature. The regression coefficient improves from 0.94 to 0.99 and the precision within one year decreases significantly by 40 % when choosing $\overline{\delta_F}$ 7 ‰ more depleted (-39 ‰ instead of -32 ‰). The precision of $\delta^{13}C(CO_2)$ -based fuel CO_2 will increase with decreasing isotopic signature of fuel CO_2 sources. Analogously, the precision of CO-based fuel CO_2 estimates will increase with decreasing inhomogeneity of CO/CO_2 ratio of fuel CO_2 sources. This effect should be taken into account when designing a measurement network and thus highlights the importance of a thorough source evaluation in the catchment area prior to instrumental installation.

List of acronyms

AMS - accelerator mass spectrometry

bf – Biofuel

bg – Background

bio – Biosphere

EDGAR- Emissions Database for Global Atmospheric Research

F – Fuel

F-bf – Fuel excluding biofuels (=ff)

ff – Fossil fuel

F-tr – Fuel excluding traffic

GC - Gas chromatography

ICOS – Integrated Carbon Observation System

IQR- Inter-quartile range

m_x – CO share of emission group x to CO offset

NPP- Nuclear power plant

ppm – parts per million, equivalent to µmol/mol

R_x – Ratio of CO to CO_2 in the emission group x

sd- Standard deviation

STILT – Stochastic Time-Inverted Langrangian Particle model

tot – Total

x- CO mole fraction

y- CO_2 mole fraction

Table 1: $\delta^{13}C(CO_2)$ source signature of fuel types and biosphere as used in the model. The isotopic signature of the biosphere follows the findings of Ballantyne et al. (2011) for Europe. The assigned isotopic fuel values were chosen from mean measured isotopic signatures in Heidelberg (Kaul, 2007 and unpublished data) or if not available, are similar to isotopic $\delta^{13}C(CO_2)$ values reported in Andres et al. (1994) or (for biogas) Widory et al. (2012).

Emission source	$\delta_{ff,i}$, $\delta_{bf,j}$ or δ_{bio} [‰]
Hard coal	-27
Brown coal	-29
Peat	-30
Solid waste	-30
Heavy oil	-31
Light oil	-31
Natural gas	-48
Derived gas	-30
Solid biomass	-29
Bio liquid	-31
Biosphere	
Jan	-27
Feb	-26
Mar	-25
Apr	-24
May	-23

Jun	-22
July	-22
Aug	-23
Sep	-24
Oct	-25
Nov	-26
Dec	-27

Table 2: Tracer or tracer combinations, required parameters and formula for estimation of targeted fuel CO_2 concentration. In cases c) and d) we further divide fuel CO_2 into traffic CO_2 and non-traffic CO_2, or fossil fuel CO_2 and biofuel CO_2, respectively. In case f) we can only estimate fossil fuel CO_2 with $\Delta^{14}C(CO_2)$and therefore lack biofuel CO_2 for a comprehensive fuel CO_2 estimate.

Case	Required parameters	Formula (for derivation see Appendix A1)
a) CO_2	-	$CO_{2F} = \Delta CO_2$
b) CO	$\overline{R_F}$	$CO_{2F} = \frac{\Delta CO}{\overline{R_F}}$
c) CO(tr) + $\delta^{13}C$-CO_2	$\overline{R_{tr}}$, $\overline{m_{tr}}$, $\overline{\delta_{tr}}$, $\overline{\delta_{F-tr}}$	$CO_{2F} = \frac{\Delta CO(t) \cdot \overline{m_{tr}}}{\overline{R_{tr}}} + \frac{CO_{2tot}\delta_{tot} - CO_{2bg}\delta_{bg} - (CO_{2tot} - CO_{2bg} - CO_{2tr})\delta_{bio} - CO_{2tr}\overline{\delta_{tr}}}{(\overline{\delta_{F-tr}} - \delta_{bio})} CO_{2tot}$
d) CO(bf) + $\delta^{13}C$-CO_2	$\overline{R_{bf}}$, $\overline{m_{bf}}$, $\overline{\delta_{bf}}$, $\overline{\delta_{ff}}$	$CO_{2F} = \frac{\Delta CO(t) \cdot \overline{m_{bf}}}{\overline{R_{bf}}} + \frac{CO_{2tot}\delta_{tot} - CO_{2bg}\delta_{bg} - (CO_{2tot} - CO_{2bg} - CO_{2tr})\delta_{bio} - CO_{2bf}\overline{\delta_{bf}}}{(\overline{\delta_{ff}} - \delta_{bio})} CO_{2tot}$
e) $\delta^{13}C$-CO_2	$\overline{\delta_F}$	$CO_{2F} = \frac{CO_{2tot}\delta_{tot} - CO_{2bg}\delta_{bg} - (CO_{2tot} - CO_{2bg})\delta_{bio}}{(\overline{\delta_F} - \delta_{bio})} CO_{2tot}$
f) $\Delta^{14}C$-CO_2	$\Delta^{14}C_{bf}$, $\Delta^{14}C_{bio}$	$CO_{2F} \approx CO_{2ff} = \frac{CO_{2bg}\left(\Delta^{14}C_{bg} - \Delta^{14}C_{bio}\right) - CO_{2tot}(\Delta^{14}C_{tot} - \Delta^{14}C_{bio}) - CO_{2bf}\left(\Delta^{14}C_{bio} - \Delta^{14}C_{bf}\right)}{(\Delta^{14}C_{bio} + 1000)}$

Table 3: Magnitude, physical reason and reference of parameter variation, which are included in Fig 5-7

Component	Variation (random)	Physical reason for variation	Reference
CO_{2meas}, CO_{2bg}	0.05 µmol/mol	Measurement uncertainty	Hammer et al., 2013
δ_{meas}, δ_{bg}	0.05 ‰	Measurement uncertainty	e.g. Tuzson et al., 2011; Vardag et al., 2015
CO offset	15 nmol/mol	natural CO sources and sinks	Gros et al., 2002; Vogel, 2010
δ_{bio}	2 ‰	heterogeneity of biosphere	cmp. to Pataki et al., 2003
$\Delta^{14}C_{meas}$, $\Delta^{14}C_{bg}$	5 ‰	Measurement uncertainty	McIntyre et al., 2013
$\Delta^{14}C_{bio}$	5 ‰	heterogeneity of biosphere and turn-over times	cmp. Taylor et al., 2015
$\Delta^{14}C_{bf}$	10 ‰	Source/Age of biofuels	--
$\overline{R_{F}}$, $\overline{R_{tr}}$, $\overline{R_{bf}}$, $\overline{\delta_{F}}$ $\overline{\delta_{ff}}$, $\overline{\delta_{bf}}$, $\overline{\delta_{tr}}$, $\overline{\delta_{F-tr}}$, $\overline{m_{bf}}$ and $\overline{m_{tr}}$	-- Submonthly variation already included as only monthly median values are used, but parameters vary at an hourly time scale	Footprint or source mix change	

Table 4: Mean difference of tracer-based estimate and modelled (as correct assumed) fuel CO_2 in µmol/mol for the tracers CO and $\delta^{13}C(CO_2)$ for different sampling strategies and respective standard deviation (both determined from a Gaussian fit to the difference histogram) for an urban setting (here: Heidelberg). Depending on the random selection of grab samples, the bias of the calibration with annualy distributed grab samples is sometimes positive and sometimes negative. Therefore, the mean absolute difference between the modelled and calibrated value was determined in a Monte-Carlo simulation and is denoted with a "±" in front of the mean value to show that the bias does not have a unique sign. The standard deviation denotes the 1-σ uncertainty of the difference, which is always bi-directional. Note, that we only show the results for CO and $\delta^{13}C(CO_2)$, since the results when using a combination of these tracers is very similar to those of the $\delta^{13}C(CO_2)$ -method. Measurement uncertainties are included in all calibration methods.

Method		CO		$\delta^{13}C$-CO_2	
		Summer	Winter	Summer	Winter
No uncertainties, monthly median values known (as shown in Fig. 1)		0.0 ± 2.1	-0.3 ± 2.0	0.0 ± 0.7	0.1 ± 1.0
Measurement uncertainties included, monthly median values known (as shown in Fig. 5)		-0.2 ± 4.3	-0.3 ± 3.7	-0.1 ± 3.5	0.0 ± 4.2
Calibration with integrated samples (method 1)	n=24	-0.8 ± 4.9	-0.7 ± 4.0	-2.4 ± 5.2	-1.8 ± 5.1
Calibration with annually distributed grab samples (method 2)	n=24	±1.2 ± 5.3	±1.5 ± 4.7	±0.8 ± 4.0	±1.6 ± 4.9
	n=96	±1.1 ± 5.2	±1.3 ± 4.5	±0.5 ± 3.8	±1.1 ± 4.5
Calibration with seasonal grab sample calibration (method 3)	n=24	±1.2 ± 5.3	±1.5 ± 4.7	±1.6 ± 4.6	±1.6 ± 4.9
	n=96	±0.8 ± 4.8	±1.1 ± 4.3	±0.9 ± 4.3	±0.8 ± 4.3
Seasonal event calibration (method 4)	n=24	±2.1± 6.1	±2.0 ± 5.1	±1.2 ± 4.3	±1.9 ± 5.1
	n=96	±1.5 ± 5.6	±1.9 ± 4.9	±1.1 ± 4.2	±1.3 ± 4.6

Table A1: Annual or half-yearly (summer = S, winter = W) averaged Δ^{14}C(CO$_2$), δ^{13}C(CO$_2$), ΔCO/ΔCO$_2$ ratios and mean fraction of CO$_2$ and CO relative to total CO$_2$ and CO offsets as used in our model study for the measurement site Heidelberg for the year 2012. Biosphere Δ^{14}C(CO$_2$) values are based on Taylor et al. (2015). The ΔCO/ΔCO$_2$ ratio and the fractions of CO$_2$ and CO offset were taken from the STILT model runs, which were fed with anthropogenic emissions from the EDGAR emission inventory. Note, that fractions of biofuels in traffic CO$_2$ emissions are not included. δ values were derived by assigning an isotopic value to each fuel type and weighting these depending on the respective share of the fuel type to total fuel CO$_2$ at the measurement site. The δ-values of the biosphere are the half-yearly mean values from Table 1. Analogously, R$_x$ (and Δ^{14}C$_x$) values were derived by assigning an emission ratio CO/CO$_2$ (and Δ^{14}C(CO$_2$)value) to each emission sector and weighting these depending on the respective share of the emission sector to total fuel CO$_2$ at the site.

Emission group	Δ^{14}C-CO$_2$ [‰]	δ^{13}C [‰]		$\bar{R}_x$= (ΔCO/ΔCO$_2$)$_x$ [ppb/ppm]	% of ΔCO$_2$		% of ΔCO	
		S	W		S	W	S	W
Fuel CO$_2$	-995	-31.5	-33.5	7	**50**	**80**	**100**	**100**
Fossil fuel CO$_2$ (excl. biofuels)	-1000	-32	-34	3	45	70	50	37
Biofuel CO$_2$	90	-27	-28	30	5	10	$\overline{m_{bf}}$ =50	$\overline{m_{bf}}$ =63
Fuel CO$_2$ excl. traffic CO$_2$ (but incl. biofuels)	-990	-31.5	-33.8	7	35	67	70	80
Traffic fuel CO$_2$	-1000	-31	-31	7	15	13	$\overline{m_{tr}}$ =30	$\overline{m_{tr}}$ =20
Biospheric CO$_2$	60	-23	-25.5	0	**50**	**20**	**0**	**0**

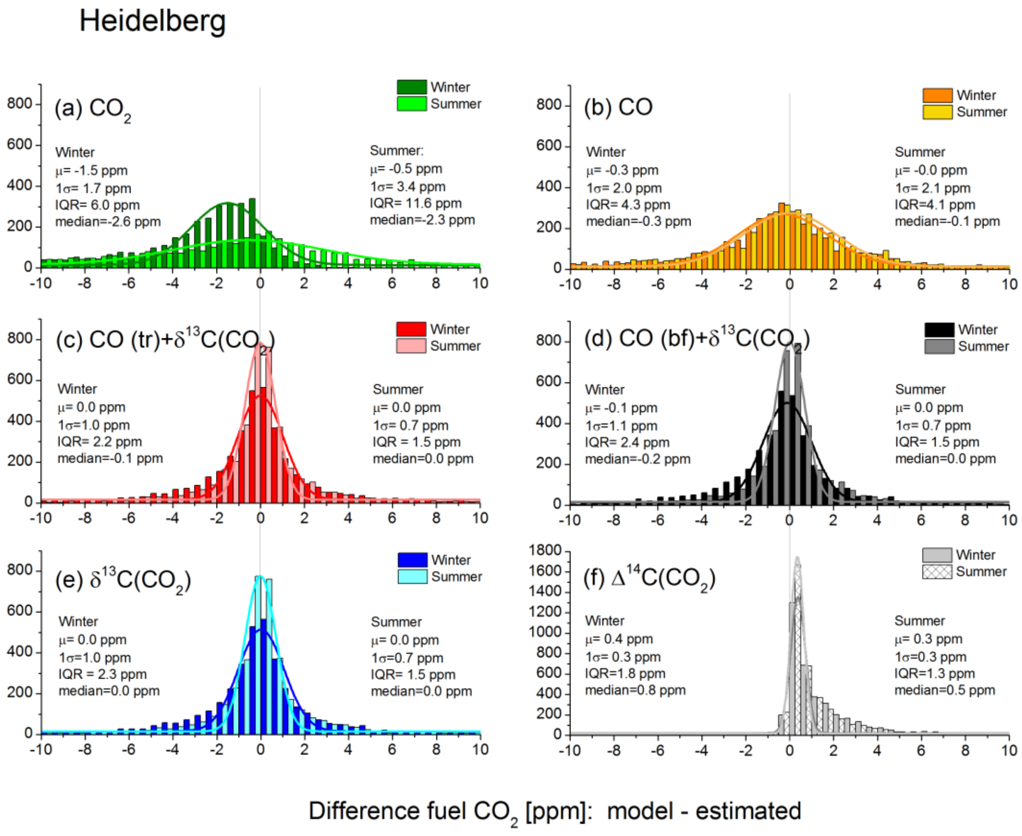

Figure 1: Histograms showing the differences between the modeled fuel CO$_2$ (assumed as correct) and the tracer-based estimated fuel CO$_2$ for the year 2012 for Heidelberg using the different tracers and tracer configurations listed in Table 2. Differences result from sub-monthly variations of parameters. Note the different y-axis scale. Darker colors denote the winter periods and lighter colors the summer periods (see legend). The distributions were fitted with a Gaussian fit and the shift (μ) and the standard deviation (σ) for the Gaussian fits are given in the figure. Since the histograms do not follow Gaussian distributions (especially for ^{14}C(CO$_2$)due to not normally distributed biofuel CO$_2$ contributions within one year) we also give the Interquartile range (IQR) in the figure to remind the reader that the uncertainty may be underestimated when using the Gaussian standard deviation for uncertainty analysis. The CO$_2$ mole fractions are given in parts per million (ppm), which is equivalent to μmol/mol. Note that in Heidelberg, mean fuel CO$_2$ for summer is 15 μmol/mol and for winter is 16 μmol/mol.

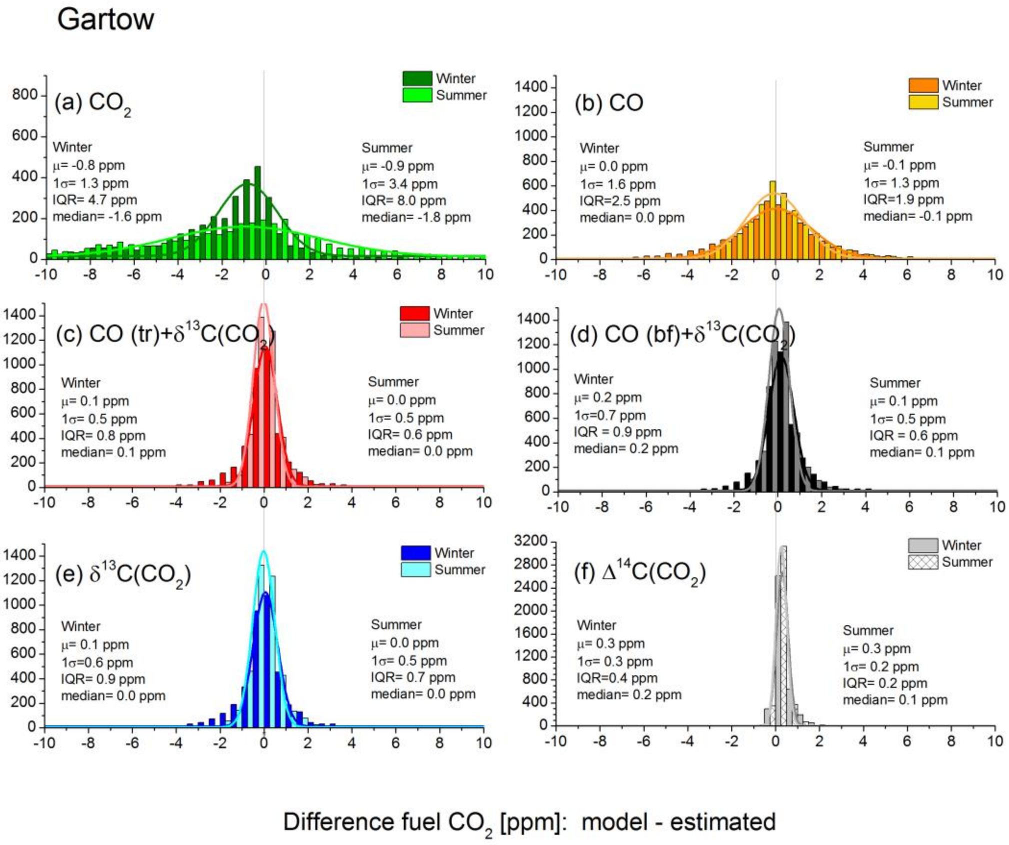

Figure 2: Same as Fig 1, but for Gartow. In Gartow, mean fuel CO$_2$ for summer is 2 μmol/mol and for winter is 4 μmol/mol.

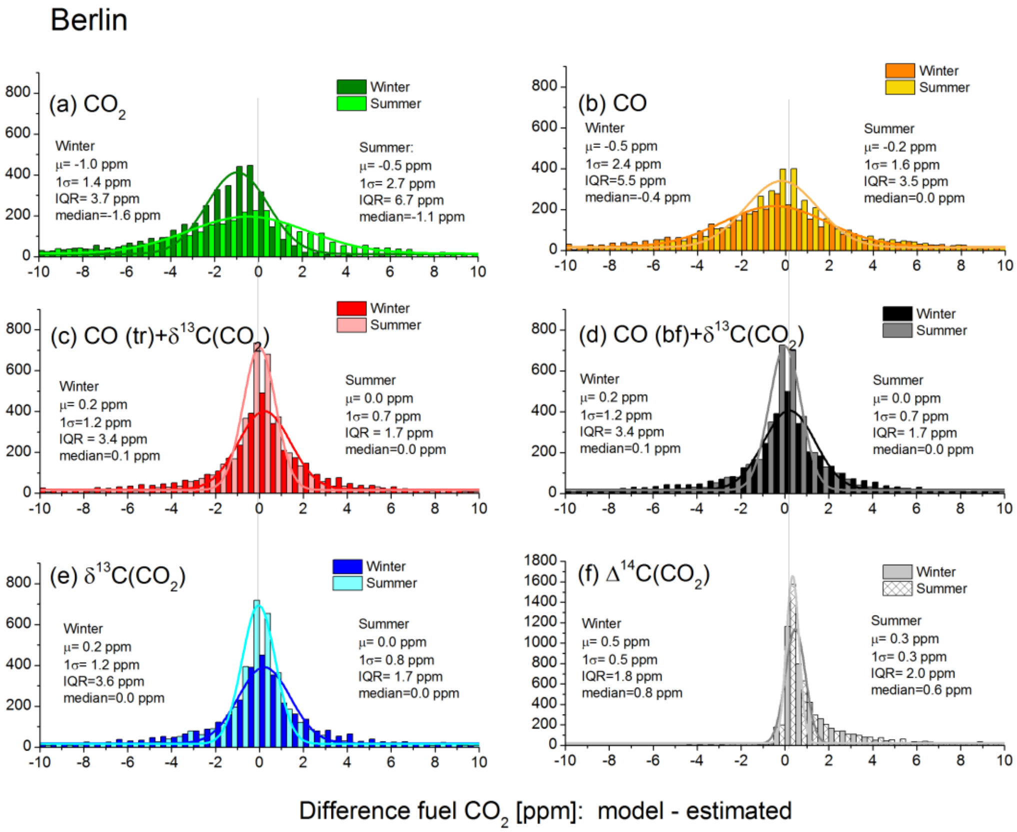

Figure 3: Same as Fig 1, but for Berlin. In Berlin, mean fuel CO_2 for summer is 23 µmol/mol and for winter is 27 µmol/mol.

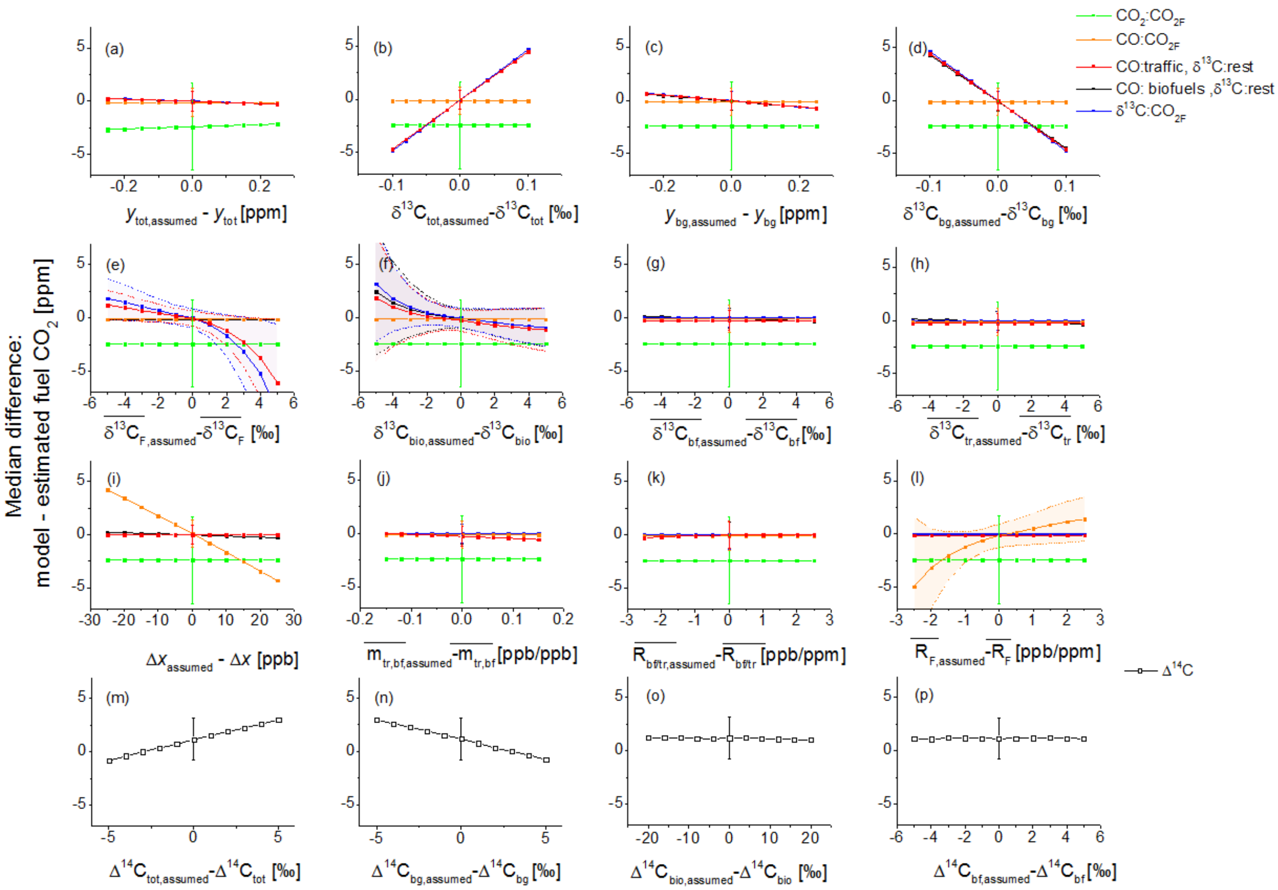

Figure 4: Sensitivity analysis: Median difference between the modelled fuel CO_2 and the tracer-based estimated fuel CO_2 value (y-axis) at a typical urban site (Heidelberg) when using parameters/variables for fuel CO_2 estimation ("assumed") deviating from the correct parameters/variables used in STILT. The error bars given at x=0 (assumed value = model value) denote the Inter-quartile ranges (IQR) for all x-positions. If the IQRs vary depending on the assumed value, the errors (IQRs) are drawn as shaded areas.

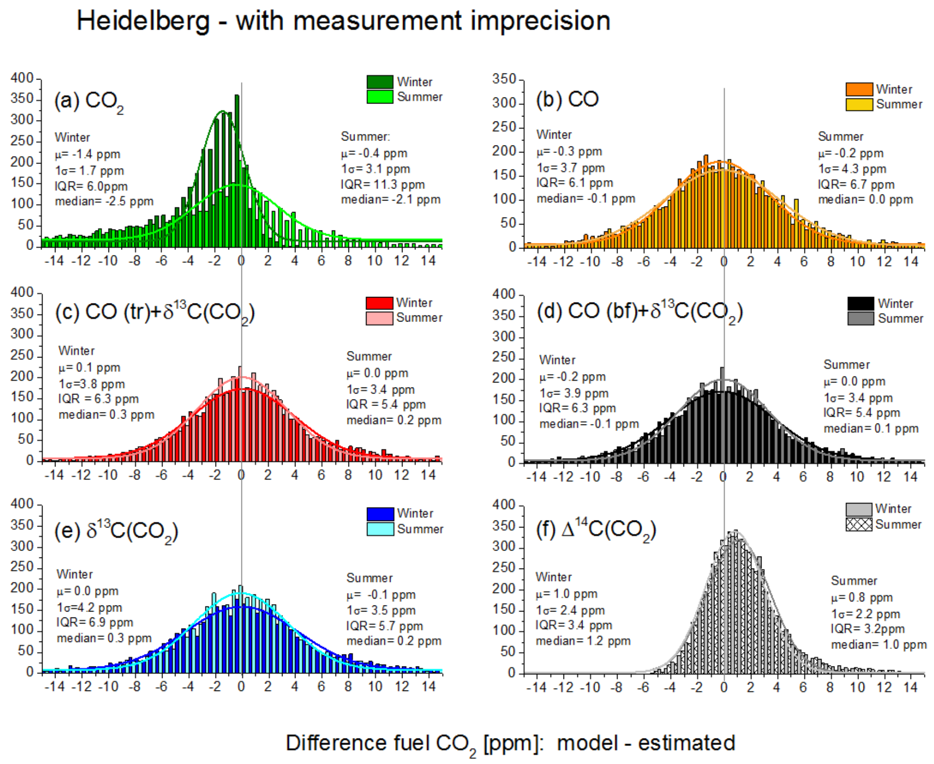

Figure 5: Same as Fig 1, but now also including measurement imprecision.

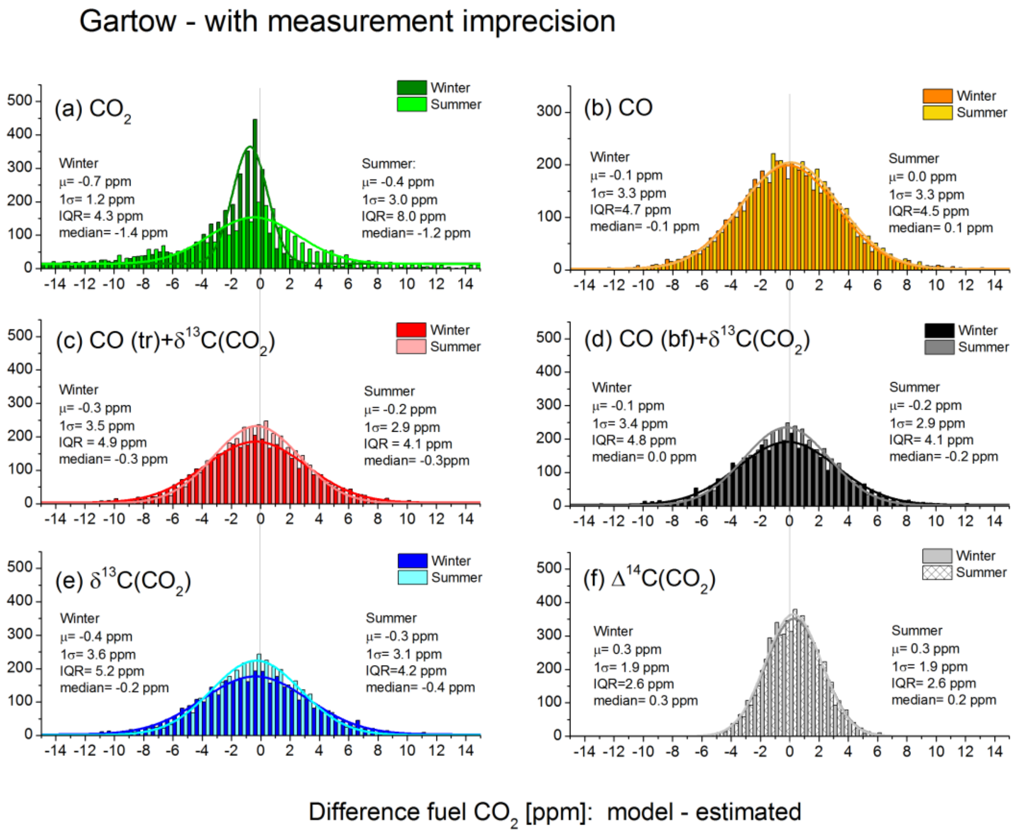

Figure 6: Same as Fig 2, but now also including measurement imprecision.

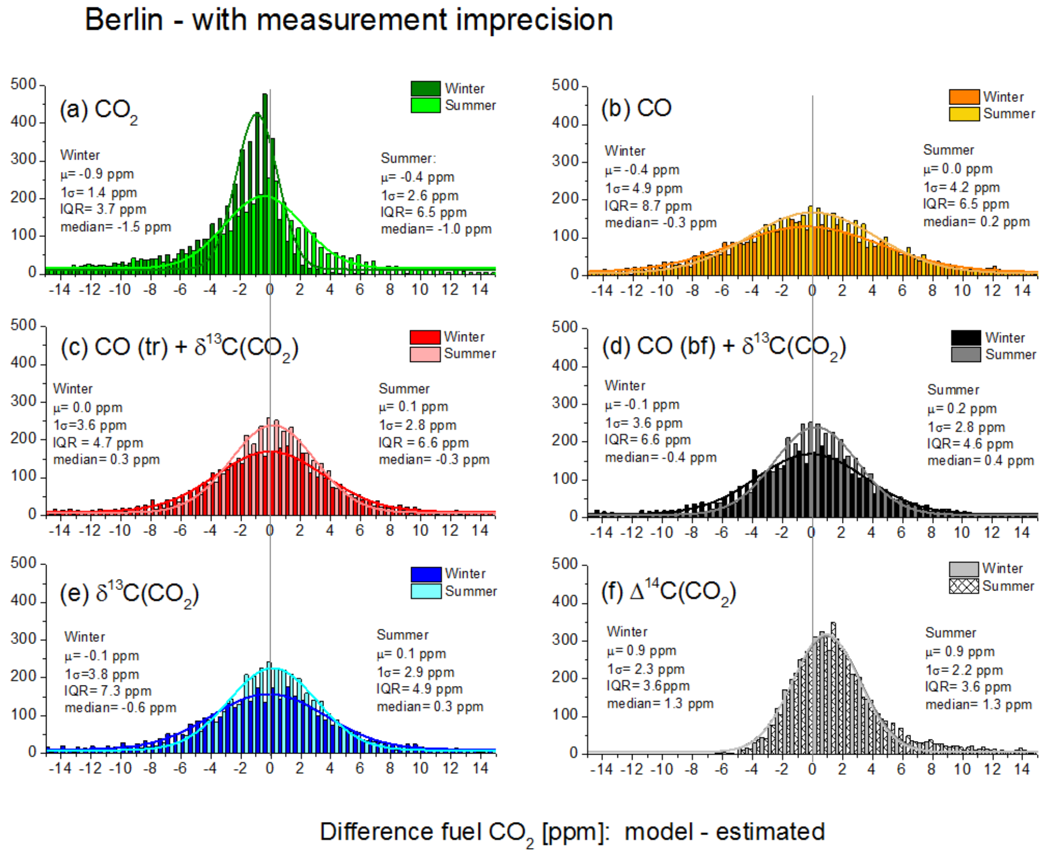

Figure 7: Same as Fig 3, but now also including measurement imprecision.

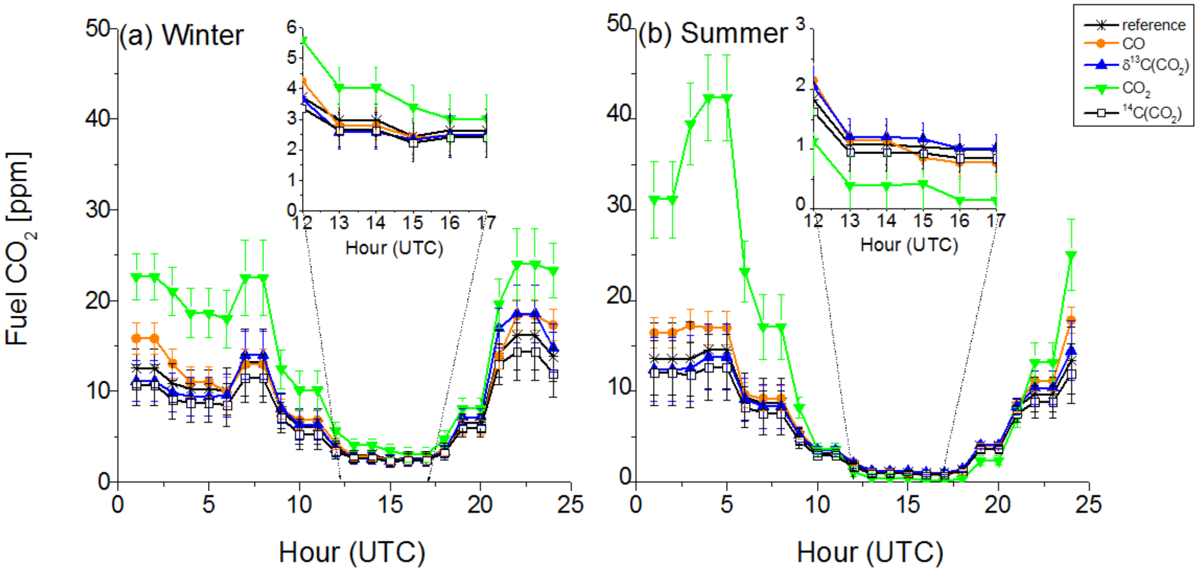

Figure 8: Comparison of median diurnal cycle of fuel CO$_2$ given in model reference or estimated with one of six different tracer methods at the measurement station Heidelberg. Error bars denote the standard error of the fuel CO$_2$ estimate at each hour for the respective half year. The diurnal cycle of the CO + δ^{13}C(CO$_2$) methods are not shown, since they are very similar to the δ^{13}C(CO$_2$) method.

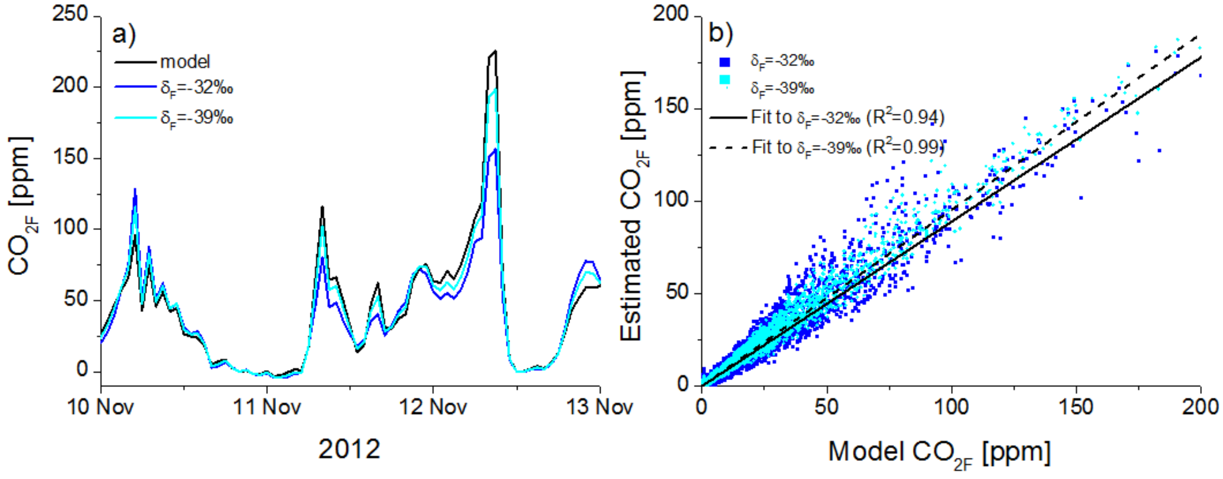

Figure A1: a) Example period showing fuel CO_2 of different fuel CO_2 estimation methods and reference modelled fuel CO_2. Dark blue: Mean δ_F is -32 ‰, cyan: mean δ_F is -39 ‰. b) Correlation plot between estimated and modelled fuel CO_2 for mean δ_F = -32 ‰ (dark blue and solid line) and mean δ_F =-39 ‰ (cyan and dotted line) during entire year 2012. Fuel CO_2 can be estimated much better using $\delta^{13}C(CO_2)$ when the fuel $\delta^{13}C$ signature is strongly depleted with respect to the biosphere. Note, that the slope slightly changes when using more depleted sources. This is because few high fuel CO_2 peaks span the linear regression and therefore determine the slope to a large degree, but as a general tendency for the Heidelberg data set the high fuel CO_2 peaks exhibit an isotopic signature, which is more enriched as the isotopic signature of the mean fuel source mix.